HHS Public Access

Author manuscript

Circulation. Author manuscript; available in PMC 2021 January 07.

Published in final edited form as:

Circulation. 2020 January 07; 141(1): 42–66. doi:10.1161/CIRCULATIONAHA.119.041460.

Critical role of cytosolic DNA and its sensing adaptor STING in aortic degeneration, dissection, and rupture

Wei Luo, MD[1,2,#], **Yidan Wang, MD, PhD**[1,2,#], **Lin Zhang, MS**[1,2], **Pingping Ren, MD, PhD**[1,2], **Chen Zhang, MD**[1,2], **Yanming Li, PhD**[1,2], **Alon R. Azares, BS**[3], **Michelle Zhang**[1], **Jiao Guo, PhD**[1,2], **Ketan B. Ghaghada, PhD**[4], **Zbigniew A. Starosolski, PhD**[4], **Kimal Rajapakshe, PhD**[5], **Cristian Coarfa, PhD**[5,6], **Yumei Li, PhD**[7], **Rui Chen, PhD**[7,8,9], **Keigi Fujiwara, PhD**[10], **Jun-ichi Abe, MD, PhD**[10], **Joseph S. Coselli, MD**[1,2,11], **Dianna M. Milewicz, MD, PhD**[12], **Scott A. LeMaire, MD**[1,2,11,*], **Ying H. Shen, MD, PhD**[1,2,11,*]

[1]Division of Cardiothoracic Surgery, Michael E. DeBakey Department of Surgery, Baylor College of Medicine, Houston, Texas, USA

[2]Department of Cardiovascular Surgery, Texas Heart Institute, Houston, Texas, USA

[3]Molecular Cardiology Research Lab, Texas Heart Institute, Houston, Texas, USA

[4]Department of Pediatric Radiology, Texas Children's Hospital, Houston, Texas, USA

[5]Department of Molecular and Cellular Biology, Baylor College of Medicine, Houston, Texas, USA

[6]Dan L. Duncan Cancer Center, Baylor College of Medicine, Houston, Texas, USA

[7]Human Genome Sequencing Center, Baylor College of Medicine, Houston, Texas, USA

[8]Department of Molecular and Human Genetics, Baylor College of Medicine, Houston, Texas, USA

[9]Department of Biochemistry and Molecular Biology, Baylor College of Medicine, Houston, Texas, USA

[10]Department of Biostatistics and Division of Internal Medicine, Department of Cardiology Research, The University of Texas MD Anderson Cancer Center, Houston, Texas, USA

[11]Cardiovascular Research Institute, Baylor College of Medicine, Houston, Texas, USA

[12]Division of Medical Genetics, Department of Internal Medicine, The University of Texas Health Science Center at Houston, Houston, Texas, USA

[*]**Correspondence** Ying H. Shen, MD, PhD, Department of Surgery, Baylor College of Medicine, One Baylor Plaza, BCM 390, Houston, Texas 77030. Phone: 832.355.9952; fax: 832.355.9951; hyshen@bcm.edu; or: Scott A. LeMaire, MD, Department of Surgery, Baylor College of Medicine, One Baylor Plaza, BCM 390, Houston, Texas 77030. Phone: 832.355.9942; fax: 832.355.9928; slemaire@bcm.edu.

[#]These authors contributed equally.

Author Contributions

The study was designed by S.A.L. and Y.H.S. The experiments were conducted by W.L., Y.W., L.Z., P.R., A.R.A., C.Z., Y.L. M.Z., J.G., K.B.G., and Z.A.S. The data were analyzed by W.L., Y.W., K.F., J.A., D.M.M., S.A.L., and Y.H.S. The single-cell RNA sequencing was performed by Y.L. (Yumei Li) and R.C., and the data analysis was performed by Y.L. (Yanming Li), K.R., C.C., W.L., Y.W. and Y.H.S. The CT images were acquired and analyzed by K.B.G. and Z.A.S. The manuscript was written by W.L., Y.W., K.F., J.A., D.M.M., J.S.C., S.A.L. and Y.H.S., and approved by all authors.

Disclosures

The authors have no potential conflicts of interest to disclose.

Abstract

BACKGROUND: Sporadic aortic aneurysm and dissection (AAD), caused by progressive aortic smooth muscle cell (SMC) loss and extracellular matrix degradation, is a highly lethal condition. Identifying mechanisms that drive aortic degeneration is a crucial step in developing an effective pharmacologic treatment to prevent disease progression. Recent evidence has indicated that cytosolic DNA and abnormal activation of the cytosolic DNA sensing adaptor STING (stimulator of interferon genes) play a critical role in vascular inflammation and destruction. Here, we examined the involvement of this mechanism in aortic degeneration and sporadic AAD formation.

METHODS: The presence of cytosolic DNA in aortic cells and activation of the STING pathway were examined in aortic tissues from patients with sporadic ascending thoracic AAD. The role of STING in AAD development was evaluated in *Sting*-deficient ($Sting^{gt/gt}$) mice in a sporadic AAD model induced by challenging mice with a combination of a high-fat diet and angiotensin II. We also examined the direct effects of STING on SMC death and macrophage activation in vitro.

RESULTS: In human sporadic AAD tissues, we observed the presence of cytosolic DNA in SMCs and macrophages and significant activation of the STING pathway. In the sporadic AAD model, $Sting^{gt/gt}$ mice showed significant reductions in challenge-induced aortic enlargement, dissection, and rupture in both the thoracic and abdominal aortic regions. Single-cell transcriptome analysis revealed that aortic challenge in wild-type mice induced the DNA damage response, the inflammatory response, dedifferentiation and cell death in SMCs, and matrix metalloproteinase (MMP) expression in macrophages. These changes were attenuated in challenged $Sting^{gt/gt}$ mice. Mechanistically, nuclear and mitochondrial DNA damage in SMCs and the subsequent leak of DNA to the cytosol activated STING signaling, which induced cell death through apoptosis and necroptosis. Interestingly, DNA from damaged SMCs was engulfed by macrophages in which it activated STING and its target IRF3, which directly induced MMP-9 expression. Importantly, pharmacologically inhibiting STING activation partially prevented AAD development.

CONCLUSIONS: Our findings indicate that the presence of cytosolic DNA and subsequent activation of cytosolic DNA sensing adaptor STING signaling is a key mechanism in aortic degeneration and that targeting STING may prevent sporadic AAD development.

Keywords

aortic aneurysm and dissection; cytosolic DNA; STING; cell death; MMP production

INTRODUCTION

Aortic aneurysm and dissection (AAD) are common interrelated cardiovascular disorders that carry a high risk of morbidity and mortality.[1] To date, no medications have been clinically proven to be effective in preventing aortic degeneration and disease progression. AAD occur either spontaneously (sporadic) or in association with a genetic condition. The key features of sporadic AAD are progressive smooth muscle cell (SMC) loss and extracellular matrix (ECM) fragmentation and depletion[2] that result in aortic aneurysm, dissection, and rupture.[2] Identifying molecules and pathways that drive SMC injury and ECM destruction is a crucial step toward developing theurapeutic targets to prevent AAD progression.

A growing body of evidence has suggested that stimulator of interferon genes (STING), a pro-inflammatory molecule in the cyclic GMP-AMP synthase (cGAS)-STING cytosolic DNA sensor signaling pathway,[3,4] plays a critical role in tissue inflammation and destruction. DNA in the cytosol binds and activates the cytosolic DNA sensor cGAS that produces cyclic GMP-AMP (cGAMP). cGAMP acts as a secondary messenger that binds and activates the adaptor STING.[3,4] Once activated, STING serves as a scaffold that recruits kinases such as tank-binding kinase 1 (TBK1) and its target proteins (e.g. interferon regulatory factor 3 [IRF3][5,6] and nuclear factor-kappa B [NF-κB][6]) and facilitates the phosphorylation and activation of IRF3 and NF-κB by TBK1. IRF3 and NF-κB then translocate into the nucleus and promote the expression of genes that facilitate immunity.[5]

STING was originally discovered as an important molecule in immunity that detects DNA from infected pathogens and triggers the immune response.[5,6] Recently, increasing evidence has indicated that abnormal STING activation plays a key role in tissue inflammation and degeneration.[7–11] Gain-of-function mutations in *STING* have been identified in patients with early onset vasculopathy and systemic inflammatory syndromes such as STING-associated vasculopathy with onset in infancy (SAVI)[9,10] and familial inflammatory syndrome with lupus-like manifestations.[8] STING can also be activated by self-DNA released from damaged nuclei or mitochondria and is implicated in tissue inflammation and damage.[7,11]

Given STING's critical role in vascular inflammation and destruction, we hypothesized that STING activation in the aortic wall induces aortic degeneration and AAD development. Here, we provide evidence showing the presence of cytosolic DNA and STING activation in aortic tissues from patients with sporadic thoracic AAD (TAAD). STING contributes to AAD development by promoting SMC apoptosis and necroptosis and by inducing matrix metalloproteinase (MMP)-9 production and ECM degradation. Importantly, we found that the pharmacologic inhibition of STING activation can reduce AAD development in mice. Our study findings suggest that the cytosolic DNA–mediated activation of cytosolic DNA sensing adaptor STING plays a critical role in aortic degeneration and is a potential therapeutic target for treating sporadic AAD.

METHODS

All data, analytic methods, and study materials will be made available to other researchers for purposes of reproducing our results or replicating the procedures. Detailed methods are provided in the online-only Data Supplement.

Human Tissue Study

The protocol for collecting human tissue samples was approved by the institutional review board at Baylor College of Medicine. Written informed consent was provided by all participants before enrollment. All experiments conducted with human tissue samples were performed in accordance with the relevant guidelines and regulations. Aortic tissue samples from patients with sporadic ascending thoracic AAD (ATAAD) and control aortic tissue samples were obtained from our existing aortic tissue bank. For detailed procedures, please refer to the online-only Data Supplement.

Animal Studies

All animal experiments were approved by the Institutional Animal Care and Use Committee at Baylor College of Medicine in accordance with the guidelines of the National Institutes of Health. To generate a mouse model of sporadic AAD, we purchased male and female WT mice (C57BL/6J) and *Sting*-deficient mice (C57BL/6J-Tmem173gt/J, or *Sting*$^{gt/gt}$) from The Jackson Laboratory (Bar Harbor, ME). For detailed procedures, please refer to the online-only Data Supplement.

Statistical Analysis

All quantitative data are presented as the mean ± standard deviation. Data were analyzed by using SPSS software, version 23.0 (SPSS Inc., Chicago, IL). For details regarding the statistical analyses, please refer to the online-only Data Supplement.

RESULTS

Presence of Cytosolic DNA and Activation of the STING Signaling Pathway in Human Sporadic ATAAD Tissues

We first examined the presence of cytosolic DNA and the activation of the STING pathway in human sporadic ATAAD tissues. Aortic tissues were collected from patients with sporadic ascending thoracic aortic aneurysm (ATAA) (n=10), patients with sporadic acute ascending thoracic aortic dissection (ATAD) (n=10), and age-matched organ donors (controls) (n=8) (Supplemental Table 1).

Western blot analyses showed that the expression and phosphorylation of STING, TBK1, and IRF3 were significantly upregulated in aortic tissues from patients with ATAA or ATAD compared with those from controls (Fig. 1A, Supplemental Figure 1A), indicating that the STING-TBK1-IRF3 pathway is activated in ATAAD tissues. Immunostaining showed that STING, TBK1, and IRF3 were highly expressed in the aortic media and adventitia of diseased aortas, particularly in SMCs in the media, CD68-positive macrophages in the adventitia (Fig. 1B), and CD68-positive cells in the media-adventitia boundary area (Supplemental Figure 1B) that may be macrophages or SMCs that underwent a pro-inflammatory phenotype switch.

Furthermore, reactive oxygen species (ROS) levels were increased in aortic tissues from patients with ATAA or ATAD compared with those from controls (Fig. 1C). Co-immunostaining of aortic tissues for double-stranded DNA (dsDNA) and the mitochondrial marker Tomm20 was used to determine the presence of cytosolic DNA that did not colocalize with nuclei or mitochondria. Compared with control tissues, patient ATAD tissues, particularly dissected tissues, had a markedly increased amount of cytosolic DNA in cells in the aortic media and adventitia (Fig. 1D), suggesting profound DNA damage and the leak of DNA to the cytosol in diseased tissues. Together, these data suggest that human sporadic ATAAD tissues are characterized by significant DNA damage, the presence of cytosolic DNA, and activation of the cytosolic DNA sensing adaptor STING pathway.

Reduction of Challenge-induced AAD Development, Aortic Degeneration, and Biomechanical Dysfunction in *Sting*-deficient Mice

We next evaluated the role of STING in aortic degeneration and AAD development by comparing disease development in WT and *Sting*-deficient (*Sting*$^{gt/gt}$) mice in a model of sporadic AAD. The *Sting*$^{gt/gt}$ mice used in our study have a point mutation (T596A) in the *Sting* gene that causes STING dysfunction and degradation.[12] In our modified[13] sporadic AAD model, mice were challenged with a combination of a high-fat diet (HFD) for 8 weeks and high-dose angiotensin II (AngII) infusion (2000 ng/min/kg) during the last 4 weeks. The use of a HFD and AngII to induce sporadic AAD represents important clinical risk factors for sporadic AAD—hypertension and dyslipidemia[14]—and reproducibly induces a spectrum of aortic pathology including dilatation, aneurysm, dissection, and rupture in different thoracic and abdominal aortic segments.[15,16] No atherosclerosis was observed in this mouse model. AngII infusion increased blood pressure similarly in WT and *Sting*$^{gt/gt}$ mice (Supplemental Figure 2A).

In WT mice challenged with a HFD and AngII, we observed marked aortic degeneration (Fig. 2A, 2B), diameter enlargement (Fig. 2C), dilatation (98%), AAD (including aortic aneurysm, dissection, and rupture; 82%), severe AAD (including dissection and rupture; 58%), and rupture (24%) (Fig. 2D). In sharp contrast to these mice, *Sting*$^{gt/gt}$ mice challenged with a HFD and Ang II showed less affected overall aortic structure (Fig. 2B), reduced aortic enlargement (Fig. 2C), and a lower incidence of AAD (33%, $P<0.001$), severe AAD (21%, $P<0.001$), and rupture (0%, $P=0.001$) (Fig. 2D). All these mice survived for the duration of the experiments (Fig. 2E); no vessel rupture occurred (Fig. 2F). Furthermore, AAD and severe AAD incidences in challenged *Sting*$^{gt/gt}$ mice were reduced in different aortic segments, particularly in the ascending aorta and suprarenal aorta (Fig. 2F). The reduced AAD incidence observed in *Sting*$^{gt/gt}$ mice was similar in males and females (Fig. 2G). To further confirm the role of STING in AAD development, we compared aortic diameter between WT and *Sting*$^{gt/gt}$ mice in a $CaCl_2$-induced abdominal aortic aneurysm (AAA) model in which calcium ion precipitates bind and disrupt elastic fibers,[17] leading to aortic destruction and AAA formation. We found that applying $CaCl_2$ to the infrarenal aorta induced aortic enlargement in WT mice (Supplemental Figure 2B and 2C), which was partially prevented in *Sting*$^{gt/gt}$ mice.

Histologic analysis showed that, compared with aortas from challenged WT mice, aortas from challenged *Sting*$^{gt/gt}$ mice had a protected aortic architecture, a preserved SMC layer, and reduced elastic fiber fragmentation (Fig. 2H). We also examined the contractile ability of the aorta in these mice. To exclude the effects of aortic fibrotic remodeling and stiffness from advanced aortic disease, we studied the biomechanical function of ascending thoracic aortas without significant gross degeneration. Wire myograph analysis showed that phenylephrine-induced aortic contraction was compromised in challenged WT mice (Fig. 2I) but preserved in challenged *Sting*$^{gt/gt}$ mice, indicating the involvement of STING in aortic contractile dysfunction. Together, these findings suggest a critical role for STING in aortic degeneration, biomechanical dysfunction, and AAD formation.

Reduction of the Challenge-induced SMC Stress Response and Macrophage Activation in *Sting*-deficient Mice

To further investigate the potential mechanisms underlying STING-mediated aortic degeneration, we examined the role of STING in challenged-induced gene expression in the aortic wall. We performed the bulk RNA-sequencing analysis of aortas isolated from unchallenged and challenged WT and $Sting^{gt/gt}$ mice one week after AngII challenge to capture the early stages of the aortic stress response. Analysis of differentially expressed genes (DEGs) revealed different gene expression patterns in aortas from unchallenged and challenged WT mice and $Sting^{gt/gt}$ mice (Fig. 3A). GO analysis showed that aortic challenge in WT mice upregulated the expression of genes involved in several biologic processes including the ROS response, DNA damage response, inflammatory response, and cell death (Fig. 3B, left panel). However, this challenge-induced gene upregulation was prevented in aortas of *Sting*-deficient mice (Fig. 3B, right panel). Furthermore, analysis of DEGs in the aortas of challenged WT mice showed the upregulation of key molecules in the STING pathway, cell death pathways (apoptosis, necroptosis, and pyroptosis), and the inflammatory response, but this challenge-induced activation was prevented in *Sting*-deficient mouse aortas (Fig. 3C).

To further examine the role of STING in challenge-induced gene expression in different aortic cell populations, we performed single-cell transcriptome analysis of aortas from unchallenged and challenged WT mice and $Sting^{gt/gt}$ mice 1 week after AngII challenge. This analysis revealed that the aortic wall was composed of 12 cell clusters (Fig. 3D), including 6 clusters of SMCs ($Acta2^{+}$, $Myh11^{+}$, $Mylk^{+}$) and 2 clusters of macrophages ($Cd68^{+}$, $Adger1^{+}$, $F13a1^{+}$). *Sting* expression was particularly high in 2 clusters of SMCs (clusters 5 and 6), 3 clusters of fibroblasts (clusters 2, 4, and 8), and one cluster of macrophages (cluster 11) (Fig. 3E, left panel). *Sting* expression in SMC clusters was induced by aortic challenge (Fig. 3E, right panel). GO enrichment analysis of one SMC cluster (cluster 5) revealed that aortic challenge in WT mice upregulated the expression of genes with roles in the ROS response, DNA damage response, inflammatory response, and cell death (Fig. 3F, upper panel). However, those challenge-induced stress responses were reduced in $Sting^{gt/gt}$ mice when compared with WT mice (Fig. 3F, lower panel). Further analysis of DEGs in this SMC cluster showed that aortic challenge also upregulated the expression of key genes in inflammation and cell death (apoptosis, necroptosis, and pyroptosis), but these challenge-induced changes were prevented in *Sting*-deficient mice (Fig. 3G). Together, our findings indicate a critical role for STING in various stress responses of aortic SMCs, including the ROS response, DNA damage response, inflammation, and cell death.

Because *Sting* was highly expressed in macrophages (cluster 11) in the aortic wall of challenged WT mice (Fig. 3E), we performed single-cell transcriptome analysis of this cluster to examine the potential role of STING in the aortic challenge–induced inflammatory response and in MMP production in macrophages. Because few macrophages were detected in the aortas of unchallenged mice, GO analysis was performed only for challenged WT and $Sting^{gt/gt}$ mice. GO analysis of this macrophage cluster revealed that the expression of genes involved in the immune response, migration, endocytosis, cytokine production, and ECM

regulation was significantly lower in the aortas of challenged *Sting*$^{gt/gt}$ mice than in those of challenge WT mice (Fig. 3H). Furthermore, the analysis of DEGs in this macrophage cluster showed that the challenge-induced expression of genes associated with ECM degradation (e.g. *Mmp2*, *Mmp8*, and *Mmp9*) and the inflammatory responses observed in WT mice was prevented in *Sting*-deficient mice (Fig. 3I).

Prevention of Challenge-induced SMC Death and Macrophage MMP Production in Aortas of *Sting*-deficient Mice

We performed further analyses of mouse aortas to confirm the findings of our transcriptome analyses and to determine the association between DNA damage and STING activation, as well as the role of STING in SMC death and macrophage activation/MMP production. In WT mice, aortic challenge markedly increased ROS production (Fig. 4A), cytosolic DNA levels (Fig. 4B and 4C), and STING activation (Fig. 4D) in the ascending aortic wall.

Furthermore, aortic challenge in WT mice also increased caspase-3 and PARP-1 cleavage (Fig. 4E), as well as the number of TUNEL-positive SMCs (Fig. 4F) in the ascending aorta. However, these apoptotic events were downregulated in *Sting*$^{gt/gt}$ mice (Fig. 4E and 4F), confirming the involvement of STING in inducing apoptosis. We also examined the effect of STING on the induction of necroptosis, which plays a critical role in the development of abdominal[18] and thoracic (data not shown) AAD. We found that aortic challenge in WT mice activated the necroptosis pathway,[19,20] as indicated by the elevated phosphorylation of receptor-interacting protein kinase 3 (RIP3)[21] and mixed lineage kinase domain-like (MLKL)[22–24] in the aortic wall (Fig. 4G), particularly in SMCs (Fig. 4H) in the ascending aorta. Importantly, the challenge-induced activation of the necroptosis pathway was reduced in *Sting*$^{gt/gt}$ mice, indicating the involvement of STING in necroptosis.

Consistent with the results of our transcriptome studies, aortic challenge in WT mice signficantly increased MMP-9 production (Fig. 4I), MMP-9 expression in macrophages (Fig. 4J), and MMP activity (Fig. 4K) in the ascending aortic wall. The challenge-induced upregulation of MMP-9 observed in the aortas of WT mice was downregulated in *Sting*$^{gt/gt}$ mice, suggesting that STING is involved in promoting MMP production and the aortic inflammatory response.

In the suprarenal aorta of WT mice challenged with a HFD and AngII, we also observed increased cytosolic DNA levels and STING activation (Supplemental Figure 3A and 3B). In addition, the suppressive effect of *Sting* deficiency on SMC apoptosis, necroptosis, and macrophage MMP-9 production was observed in the suprarenal aorta (Supplemental Figures 3B-3D).

Together, these findings suggest that STING may contribute to aortic degeneration and AAD formation in part by promoting SMC death and macrophage MMP-9 production.

Activation of the STING-TBK1-IRF3 Pathway in Aortic SMCs by ROS-induced DNA Damage and the Release of DNA into the Cytosol

To further determine whether cytosolic DNA and STING signaling play a direct role in promoting SMC death, we performed a series of experiments using cultured aortic SMCs.

We used H_2O_2, a potent inducer of cell dysfunction and death, to trigger DNA damage and STING activation. Treating SMCs with H_2O_2 induced a marked increase in the accumulation of small dsDNA particles outside nuclei, mitochondria, and lysosomes (Fig. 5A), which is indicative of the presence of cytosolic DNA. The additional quantification of DNA in the cytosolic fraction showed a significant increase in the amount of cytosolic dsDNA in H_2O_2-treated SMCs (Fig. 5B). Moreover, H_2O_2 consistently and dose-dependently increased the phosphorylation of STING, TBK1, and IRF3 (Fig. 5C, Supplemental Figure 4A) in cultured SMCs, indicating activation of this DNA sensing pathway. Furthermore, transfecting SMCs with exogenous DNA[25] isolated from H_2O_2-treated SMCs directly increased the phosphorylation of STING, TBK1, and IRF3 (Fig. 5D, Supplemental Figure 4B). Together, these data support the possibility that ROS cause DNA damage and the release of DNA fragments into the cytosol, subsequently activating the STING-TBK1-IRF3 signaling pathway.

Critical Role of the STING-TBK1-IRF3 Pathway in Aortic SMC Death

We examined whether the STING-TBK1-IRF3 pathway is involved in SMC death. Flow cytometry analyses showed that treating SMCs with H_2O_2[18,26,27] for 24 hours or transfecting SMCs with exogenous SMC DNA[28,29] induced cell death (Fig. 5E), which was partially reduced by knocking down *STING*, *TBK1*, or *IRF3* with siRNA, indicating the involvement of this pathway in H_2O_{2-} or exogenous DNA–induced SMC death.

We then examined the role of the STING-TBK1-IRF3 pathway in SMC necroptosis and apoptosis. To focus on necroptosis, we blocked apoptosis with zVAD.[21,22,24] Adding H_2O_2 or exogenous SMC DNA to zVAD-pretreated SMCs induced cell death (Fig. 5F), which was reduced by knocking down *STING*, *TBK1*, or *IRF3*, suggesting the involvement of this pathway in apoptosis-independent SMC death. H_2O_2 or exogenous SMC DNA also dose-dependently increased the phosphorylation of RIP3 and MLKL (Fig. 5G, Supplemental Figure 4C), indicating that these treatments activate the necroptosis pathway. Importantly, knocking down *STING*, *TBK1*, or *IRF3* reduced RIP3 and MLKL phosphorylation (Fig. 5H, Supplemental Figure 4D), whereas overexpressing STING and TBK1 increased RIP3 and MLKL phosphorylation (Fig. 5I, Supplemental Figure 4E).

We also examined the role of STING in SMC apoptosis. Treating SMCs with H_2O_2 or transfecting them with exogenous SMC DNA induced caspase-3 and PARP-1 cleavage (Supplemental Figure 4F) and increased apoptotic SMC death (Supplemental Figure 4G), which was partially prevented by knocking down *STING*, *TBK1*, or *IRF3*.

Together, these findings indicate that the STING-TBK1-IRF3 signaling pathway plays a critical role in SMC necroptosis and apoptosis induced by ROS and cytosolic DNA.

Activation of the STING-IRF3 Signaling Pathway in Macrophages by DNA from Damaged SMCs

Aortic injury triggers inflammatory responses, which in turn cause further aortic injury and ECM destruction. Although the effects of this vicious cycle on AAD progression have been well established, the molecular process of its initiation remains poorly understood. During tissue damage, injured cells release a large amount of danger molecules that induce a

profound inflammatory response.[30] Because free DNA is a proinflammatory molecule, we asked whether damaged aortic SMCs release DNA, which then activates inflammatory cells.

To test this scenario *in vitro*, we developed a SMC-macrophage co-culture system. Aortic SMCs were labeled with the DNA dye EdU (5-ethynyl-2'-deoxyuridine), washed, and treated with H_2O_2 before being co-cultured with macrophages in a transwell with SMCs on the insert membrane and macrophages on the well surface (Fig. 6A). As depicted in Figure 6A, the assay detects labeled DNA (green) released from SMCs.

Indeed, we observed small SMC-derived DNA particles in the cytosol of macrophages (Fig. 6B), indicating that macrophages had phagocytosed DNA from injured SMCs. We also observed significantly increased STING activation and MMP-9 production in macrophages that were co-cultured with H_2O_2 -treated SMCs compared with macrophages that were co-cultured with untreated SMCs (Fig. 6C, Supplemental Figure 5A). Because DNA from injured cells[27,29] can be transferred to macrophages in free form or in exosomes,[31] we determined the contribution of free SMC DNA in macrophage activation by digesting free DNA with DNase I in the coculture system. DNase I partially reduced the induction of STING activation and MMP-9 production in macrophages (Supplemental Figure 5B), suggesting that macrophage activation is partly mediated by free DNA, most likely from damaged and dead SMCs.

Further studies showed that treating macrophages with DNA[29] isolated from H_2O_2-treated SMCs induced STING and IRF3 phosphorylation (Fig. 6D, Supplemental Figure 5C), as well as STING perinuclear translocation and IRF3 nuclear translocation (Supplemental Figure 5D), indicating STING-IRF3 pathway activation in macrophages by DNA derived from injured aortic SMCs. Treating macrophages with SMC-derived DNA also increased the expression of MMP-9 protein (Fig. 6E, Supplemental Figure 5E) and *MMP9* mRNA (Fig. 6F) and increased MMP activity (Fig. 6G).

Critical Role of the STING-IRF3 Pathway in Macrophage MMP-9 Production Induced by SMC-derived DNA

We examined whether STING and IRF3 are involved in macrophage MMP-9 production induced by DNA from injured aortic SMCs. Knocking down *STING* or *IRF3* prevented the SMC DNA–induced increase in the levels of MMP-9 protein (Fig. 6H, Supplemental Figure 5F), *MMP9* mRNA (Fig. 6I), and MMP activity (Fig. 6J). Conversely, overexpressing STING or IRF3 increased the levels of MMP-9 protein (Fig. 6H, Supplemental Figure 5G), *MMP9* mRNA (Fig. 6I), and MMP activity (Fig. 6J). These results show that the STING-IRF3 pathway plays a critical role in macrophage MMP-9 production.

To investigate whether IRF3 has a direct role in *MMP9* transcription, we studied the structure of the *MMP9* gene and found that the 5′ untranslated region contains several putative IRF3 binding sites[32] (Supplemental Figure 5H). Chromatin immunoprecipitation analyses showed that IRF3 directly bound the *MMP9* promoter and that this binding was triggered by treating macrophages with SMC-derived DNA (Fig. 6K) and was prevented by silencing STING expression (Fig. 6K, Supplemental Figure 5I). Collectively, our findings suggest that the STING-IRF3 signaling pathway in macrophages may sense engulfed DNA

from injured SMCs and subsequently trigger MMP-9 production, thereby contributing to ECM degradation.

Association of STING Activation with SMC Injury and MMP-9 Production in Human Sporadic ATAAD Tissues

In aortas from ATAAD patients, we often observed profound SMC death by necrosis (characterized by disrupted cell membranes with swelling of nuclei, mitochondria, and endoplasmic reticulum) and by apoptosis (characterized by the blebbing of cell membranes with cell shrinkage, nuclear fragmentation, and chromatin condensation) (Fig. 7A). Consistent with this, we detected significant necroptosis pathway activation[19,20] in these areas, as indicated by elevated expression and phosphorylation of RIP3[21] and MLKL[22–24] (Fig. 7B, Supplemental Figure 6A) and elevated levels of phosphorylated RIP3 and MLKL in SMCs (Fig. 7C, Supplemental Figure 6B). Similarly, compared with normal aortas, diseased aortic tissues showed increased TUNEL-positive apoptotic SMCs (Supplemental Figure 6C) and cleaved caspase-3 and PARP-1 (Supplemental Figure 6D and 6E), particularly in areas with significant tissue degeneration. Importantly, activation of the STING-TBK1-IRF3 signaling pathway was correlated with activation of the necroptosis (Fig. 7B vs. Fig. 1A) and apoptosis (Supplemental Figure 6D vs. Fig. 1A) pathways in the same set of patient tissues (Supplemental Figure 6F and 6G). Furthermore, STING colocalized with the phosphorylated form of RIP3 and MLKL in SMCs of diseased aortic tissues (Fig. 7D), showing a correlation between STING-TBK1 activation and necroptosis in SMCs in human ATAAD.

Diseased aortic tissues also contained significantly elevated levels of MMP-9 (Fig. 7E, Supplemental Figure 6H) compared with control tissues. Again, STING signaling pathway activation (Fig. 7E vs. Fig. 1A) was correlated with MMP-9 production in the same set of diseased aortic tissues (Supplemental Figure 6I). Immunostaining results showed increased MMP-9 levels in macrophages of diseased aortic tissues (Fig. 7F). STING and IRF3 colocalized with MMP-9 in macrophages of the diseased area of aortic tissues (Fig. 7G), indicating an association between STING-IRF3 activation and MMP-9 production in the macrophages of ATAAD tissues.

Prevention of Aortic Degeneration and AAD Development in HFD-Ang II–Challenged WT Mice Treated with TBK1 Inhibitor Amlexanox

Having established the importance of STING in AAD development, we investigated whether aortic degeneration and AAD progression could be prevented by pharmacologically inhibiting STING activation in mice. Because the full activation of STING requires its phosphorylation at serine 366 by kinase TBK1,[33] blocking TBK1 with an inhibitor is an effective approach to preventing STING activation. Amlexanox, a clinically proven small anti-inflammatory molecule,[34,35] is the most well-studied TBK1 inhibitor and has a high affinity and specificity for TBK1[36] and inhibitor-κB kinase ε (IKK-ε)/nuclear factor kappa-light-chain-enhancer of activated B cells (NFκB).

When we treated SMCs with amlexanox, it partially prevented the effects of H_2O_2 and exogenous SMC DNA, including STING and IRF3 phosphorylation (Supplemental Figure

7A), SMC necroptosis, RIP3 and MLKL phosphorylation, and caspase-3 cleavage (Supplemental Figure 7B-7D). In macrophages, amlexanox partially prevented SMC DNA–induced increases in MMP-9 protein level, *MMP9* mRNA level, and MMP activity (Supplemental Figure 7E-7G). These findings support that amlexanox prevents STING pathway activation, SMC death, and macrophage activation.

We examined the effects of amlexanox on reducing AAD development and progression in our mouse model of sporadic AAD. WT mice were challenged with a HFD and AngII infusion and also received either amlexanox (100 mg per kg) or sunflower oil (control) during AngII infusion. Compared with the control-treated mice, mice treated with amlexanox showed better preserved aortic structure (Fig. 8A); less aortic enlargement (Fig. 8B); significantly reduced incidences of AAD (45%, $p<0.001$), severe AAD (22%, $p<0.001$), and rupture (0%, $P = 0.02$) (Fig. 8C); and an improved survival rate (Fig. 8D). Reduced AAD incidence was observed in different aortic regions in the HFD-AngII–challenged mice treated with amlexanox, particularly in the ascending and suprarenal segments (Fig. 8E). The disease reduction by amlexanox was similar in male and female mice (Fig. 8F). Consistent with our studies of gross aortic structure (Fig. 8A), we observed better preserved elastic fiber architecture in the aortas of the HFD-Ang II–challenged mice treated with amlexanox than in those of the challenged mice without amlexanox treatment (Fig. 8G). Additionally, the challenge-induced increases in STING and IRF3 phosphorylation (Supplemental Figure 7H), RIP3 and MLKL phosphorylation (Fig. 8H), the number of TUNEL-positive cells (Fig. 8I), and the production of MMP-9 (Fig. 8J) were reduced in the aortic wall of mice treated with amlexanox. These data clearly indicate a protective effect of amlexanox against aortic degeneration and AAD formation.

DISCUSSION

AAD is a highly lethal condition; thus, identifying therapeutic targets to prevent disease progression is critical. Recently, a growing body of evidence has suggested that STING signaling plays a central role in tissue destruction and inflammation in numerous diseases such as autoimmune diseases,[7,8] alcoholic liver injury,[11] and vascular inflammation and degeneration.[7,9,25] In this study, we observed the presence of cytosolic DNA and activation of the STING signaling pathway in aortic tissues from patients with sporadic ATAAD, particularly in SMCs and macrophages. Using a previously developed mouse model of sporadic AAD in which mice were challenged with a HFD and AngII,[15,16] we showed that aortic challenge in WT mice induced aortic degeneration, biomechanical dysfunction, aneurysm and dissection formation, and rupture and that these effects were significantly reduced in the aortas of *Sting*$^{gt/gt}$ mice. This was observed in different thoracic and abdominal aortic segments in both male and female mice. Furthermore, aortic tissues from challenged *Sting*$^{gt/gt}$ mice showed reduced levels of SMC apoptosis and necroptosis, a diminished inflammatory response, and reduced MMP-9 production and activity. In cultured SMCs, cellular injury and the subsequent release of DNA into the cytosol activated the STING-TBK1-IRF3 pathway, which promoted SMC apoptosis and necroptosis. In cultured macrophages, DNA released from damaged SMCs activated STING and its target IRF3, which bound to the *MMP9* promoter and stimulated MMP-9 production. Finally, we showed that pharmacologically inhibiting STING activation with amlexanox partially alleviated

aortic degeneration and AAD development in mice. These findings suggest that STING is a novel, critical molecule involved in aortic degeneration and sporadic AAD formation. However, further studies are needed to establish STING's role in the progression of genetically triggered TAADs.

STING may induce aortic degeneration through several mechanisms. Our transcriptome analyses of mouse aortas suggest that STING is involved in inducing multiple stress responses in SMCs including the oxidative stress response, the DNA damage response, the inflammatory response, and activation of cell death pathways. We provide supporting evidence that SMC apoptosis and necroptosis represent important mechanisms by which the STING pathway promotes aortic degeneration. STING and IRF3 have previously been shown to promote apoptosis[11] and necroptosis[37] partially through type I IFN and tumor necrosis factor receptor signaling.[37,38] In addition, our unpublished findings suggest that TBK1 may directly phosphorylate RIP3 to activate the necroptosis pathway. Thus, the STING pathway may induce different types of cell death through multiple direct or indirect mechanisms. Our findings also reveal that macrophage MMP-9 production and ECM degradation represent another potential mechanism for STING-mediated AAD formation. Moreover, we observed profound cytosolic DNA in SMCs of aortic tissues from patients with sporadic ATAAD. The cytosolic DNA in AAD is most likely self-DNA leaked from damaged nuclei[39] or mitochondria[40,41] in aortic cells.[3] The question remains, what are the triggers in AAD that cause nuclear and mitochondrial DNA damage and leakage? We observed significantly increased intracellular ROS levels in aortic tissues from ATAAD patients, which could be one cause of DNA damage and leakage. Further studies are required to identify other triggers so that we can develop ways to prevent cytosolic DNA generation and accumulation.

During AAD development, damaged aortic cells release a large amount of danger molecules that activate inflammatory cells, which in turn secrete enzymes (e.g. MMPs) that digest ECM and trigger further aortic damage.[30] Our study findings indicate that cytosolic DNA and the cytosolic DNA sensor mechanism are a link between SMC injury and macrophage activation in the aortic wall. We found that macrophages engulfed DNA released from injured SMCs. Furthermore, the SMC-derived DNA in macrophages activated STING and subsequently its target IRF3, which entered the nucleus, bound to the *MMP9* promoter, and induced MMP-9 expression. In challenged $Sting^{gt/gt}$ mice, MMP-9 production and elastic fiber degradation were significantly reduced. Our findings are consistent with those of recent reports supporting the role of DNA from damaged tissues in macrophage activation.[27–29] However, understanding the process that occurs from DNA uptake to STING activation requires further investigation.

It is important to note that the mechanism of inflammatory cell activation by SMC-derived DNA is best applied to AAD with significant inflammation, including inflammatory sporadic TAAD and AAA. This DNA-mediated SMC-macrophage crosstalk most likely occurs locally in areas with inflammatory cell infiltration (e.g. the media and media-adventitia boundary area). One intriguing question that remains is how DNA released from SMCs in the aortic media becomes accessible to macrophages in the adventitia and activates them. Interestingly, recent studies have shown evidence of neo-angiogenesis in human

TAAD tissues in which newly formed vessels in the adventitia cross the full thickness of the media.[42,43] Because DNA from dead cells can enter the circulation, particularly when there is significant tissue damage and increased permeability of small vessels,[44–46] DNA released from SMCs in the media may conceivably travel through the pathologic vasa vasorum and reach macrophages in the adventitia. Further studies are warranted to examine this possibility.

Finally, we assessed the therapeutic potential of targeting STING with amlexanox to treat AAD. Amlexanox is a high-affinity TBK1 inhibitor[36], which directly phosphorylates STING and facilitates its activation. Amlexanox has been used to treat aphthous ulcers (as a topical paste)[34,35] and asthma,[47] and its anti-inflammatory effects have recently generated interest in repurposing this drug for other diseases. Amlexanox has also been shown to reduce inflammation and tissue degeneration in mouse models of disease including diabetes,[36,48] neuroinflammation,[49] hepatic steatosis.[50] Using our mouse model of sporadic AAD, we found that amlexanox treatment partially prevented AAD development, supporting that the targeting of STING may be a novel strategy for preventing tissue degeneration, inflammation, and disease progression in patients with AAD. Further studies are warranted to develop direct and specific STING inhibitors. Given the crucial role of STING in fighting against pathogens and infections, STING levels must be delicately balanced in patients with careful timing and dosing of STING inhibitor treatment.

In conclusion, our findings indicate that DNA damage, cytosolic DNA, and the cytosolic DNA sensing adaptor STING play a critical role in aortic degeneration and AAD formation by promoting SMC injury, macrophage MMP production, and ECM degeneration (Fig. 8K). STING may represent a novel potential therapeutic target for treating aortic diseases.

Supplementary Material

Refer to Web version on PubMed Central for supplementary material.

Acknowledgments

We gratefully acknowledge Nicole Stancel, PhD, ELS(D), of Scientific Publications at the Texas Heart Institute, for editorial support, and Scott Weldon, MA, at Division of Cardiothoracic Surgery, Baylor College of Medicine for creating illustration. We would like to acknowledge Dr. Yun Mao and Chris Guardado in the Department of Surgery at Baylor College of Medicine for technical support, and Dr. Ananth Annapragada and Dr. Eric Tanifum in the Department of Pediatric Radiology at Texas Children's Hospital and Texas Children's Hospital Small Animal Imaging Facility for micro-CT imaging.

Funding Sources

This study was supported by National Institutes of Health (NIH) grants R01HL131980, R01HL143359, R01 HL127111, HL-130193, HL-123346, and HL-118462 and American Heart Association grants 15GRNT23040007, 18SFRN33960114, and 19CSLOI34660145. Transcriptome analyses were performed at the Department of Molecular and Human Genetics Functional Genomics Core and Single Cell Genomics Core at Baylor College of Medicine, which are partially supported by NIH grants S10OD023469, S10OD018033, S10OD025240, CA125123, and 1P30ES030285 and Cancer Prevention Research Institute of Texas core grant RP170005.

NONSTANDARD ABBREVIATIONS AND ACRONYMS

AAA	abdominal aortic aneurysm

AAD	aortic aneurysm and dissection
AngII	angiotensin II
ATAA	ascending thoracic aortic aneurysm
ATAAD	ascending thoracic aortic aneurysm and dissection
ATAD	ascending thoracic aortic dissection
CTA	computed tomography angiography
cGAS	cyclic GMP-AMP synthase
cGAMP	cyclic GMP-AMP
DEG	differentially expressed genes
dsDNA	double-stranded DNA
ECM	extracellular matrix
GO	gene ontology
H&E	hematoxylin and eosin
HFD	high-fat diet
IKK-ε	inhibitor-κB kinase ε
IRF3	interferon regulatory factor 3
MLKL	mixed lineage kinase domain-like
MMP	matrix metalloproteinase
mtDNA	mitochondrial DNA
NF-κB	nuclear factor-kappa B
ROS	reactive oxygen species
SAVI	STING-associated vasculopathy with onset in infancy
SMC	smooth muscle cell
STING	stimulator of interferon genes
TAAD	thoracic aortic aneurysm and dissection
TUNEL	terminal deoxynucleotidyl transferase dUTP nick-end labeling
TBK1	tank-binding kinase 1

REFERENCES

1. Minino AM, Murphy SL, Xu J, Kochanek KD. Deaths: final data for 2008. Natl Vital Stat Rep. 2011;59:1–126.
2. Guo DC, Papke CL, He R, Milewicz DM. Pathogenesis of thoracic and abdominal aortic aneurysms. Ann N Y Acad Sci. 2006;1085:339–352. [PubMed: 17182954]
3. Ablasser A, Goldeck M, Cavlar T, Deimling T, Witte G, Rohl I, Hopfner KP, Ludwig J, Hornung V. cGAS produces a 2'−5'-linked cyclic dinucleotide second messenger that activates STING. Nature. 2013;498:380–384. [PubMed: 23722158]
4. Wu J, Sun L, Chen X, Du F, Shi H, Chen C, Chen ZJ. Cyclic GMP-AMP is an endogenous second messenger in innate immune signaling by cytosolic DNA. Science. 2013;339:826–830. doi: 10.1126/science.1229963. [PubMed: 23258412]
5. Holm CK, Jensen SB, Jakobsen MR, Cheshenko N, Horan KA, Moeller HB, Gonzalez-Dosal R, Rasmussen SB, Christensen MH, Yarovinsky TO, Rixon FJ, Herold BC, Fitzgerald KA, Paludan SR. Virus-cell fusion as a trigger of innate immunity dependent on the adaptor STING. Nat Immunol. 2012;13:737–743. [PubMed: 22706339]
6. Ishikawa H, Barber GN. STING is an endoplasmic reticulum adaptor that facilitates innate immune signalling. Nature. 2008;455:674–678. [PubMed: 18724357]
7. Ahn J, Gutman D, Saijo S, Barber GN. STING manifests self DNA-dependent inflammatory disease. Proc Natl Acad Sci U S A. 2012;109:19386–19391. [PubMed: 23132945]
8. Jeremiah N, Neven B, Gentili M, Callebaut I, Maschalidi S, Stolzenberg MC, Goudin N, Fremond ML, Nitschke P, Molina TJ, Blanche S, Picard C, Rice GI, Crow YJ, Manel N, Fischer A, Bader-Meunier B, Rieux-Laucat F. Inherited STING-activating mutation underlies a familial inflammatory syndrome with lupus-like manifestations. J Clin Invest. 2014;124:5516–5520. doi: 10.1172/JCI79100. [PubMed: 25401470]
9. Liu Y, Jesus AA, Marrero B, Yang D, Ramsey SE, Montealegre Sanchez GA, Tenbrock K, Wittkowski H, Jones OY, Kuehn HS, Lee CC, DiMattia MA, Cowen EW, Gonzalez B, Palmer I, DiGiovanna JJ, Biancotto A, Kim H, Tsai WL, Trier AM, Huang Y, Stone DL, Hill S, Kim HJ, St Hilaire C, Gurprasad S, Plass N, Chapelle D, Horkayne-Szakaly I, Foell D, Barysenka A, Candotti F, Holland SM, Hughes JD, Mehmet H, Issekutz AC, Raffeld M, McElwee J, Fontana JR, Minniti CP, Moir S, Kastner DL, Gadina M, Steven AC, Wingfield PT, Brooks SR, Rosenzweig SD, Fleisher TA, Deng Z, Boehm M, Paller AS, Goldbach-Mansky R. Activated STING in a vascular and pulmonary syndrome. N Engl J Med. 2014;371:507–518. [PubMed: 25029335]
10. Munoz J, Rodiere M, Jeremiah N, Rieux-Laucat F, Oojageer A, Rice GI, Rozenberg F, Crow YJ, Bessis D. Stimulator of interferon genes-associated vasculopathy with onset in infancy: A mimic of childhood granulomatosis with polyangiitis. JAMA Dermatol. 2015;151:872–877. doi: 10.1001/jamadermatol.2015.0251. [PubMed: 25992765]
11. Petrasek J, Iracheta-Vellve A, Csak T, Satishchandran A, Kodys K, Kurt-Jones EA, Fitzgerald KA, Szabo G. STING-IRF3 pathway links endoplasmic reticulum stress with hepatocyte apoptosis in early alcoholic liver disease. Proc Natl Acad Sci U S A. 2013;110:16544–16549. [PubMed: 24052526]
12. Sauer JD, Sotelo-Troha K, von Moltke J, Monroe KM, Rae CS, Brubaker SW, Hyodo M, Hayakawa Y, Woodward JJ, Portnoy DA, Vance RE. The N-ethyl-N-nitrosourea-induced Goldenticket mouse mutant reveals an essential function of Sting in the in vivo interferon response to Listeria monocytogenes and cyclic dinucleotides. Infect Immun. 2011;79:688–694. doi: 10.1128/IAI.00999-10. [PubMed: 21098106]
13. Daugherty A, Manning MW, Cassis LA. Angiotensin II promotes atherosclerotic lesions and aneurysms in apolipoprotein E-deficient mice. J Clin Invest. 2000;105:1605–1612. doi: 10.1172/JCI7818. [PubMed: 10841519]
14. Sidloff D, Choke E, Stather P, Bown M, Thompson J, Sayers R. Mortality from thoracic aortic diseases and associations with cardiovascular risk factors. Circulation. 2014;130:2287–2294. doi: 10.1161/CIRCULATIONAHA.114.010890. [PubMed: 25394733]
15. Gulen MF, Koch U, Haag SM, Schuler F, Apetoh L, Villunger A, Radtke F, Ablasser A. Signalling strength determines proapoptotic functions of STING. Nat Commun. 2017;8:427. doi: 10.1038/s41467-017-00573-w. [PubMed: 28874664]

16. Wu D, Ren P, Zheng Y, Zhang L, Xu G, Xie W, Lloyd EE, Zhang S, Zhang Q, Curci JA, Coselli JS, Milewicz DM, Shen YH, LeMaire SA. NLRP3 (nucleotide oligomerization domain-like receptor family, pyrin domain containing 3)-caspase-1 inflammasome degrades contractile proteins: implications for aortic biomechanical dysfunction and aneurysm and dissection Formation. Arterioscler Thromb Vasc Biol. 2017;37:694–706. doi: 10.1161/ATVBAHA.116.307648. [PubMed: 28153878]

17. Chiou AC, Chiu B, Pearce WH. Murine aortic aneurysm produced by periarterial application of calcium chloride. J Surg Res. 2001;99:371–376. doi: 10.1006/jsre.2001.6207. [PubMed: 11469913]

18. Wang Q, Liu Z, Ren J, Morgan S, Assa C, Liu B. Receptor-interacting protein kinase 3 contributes to abdominal aortic aneurysms via smooth muscle cell necrosis and inflammation. Circ Res. 2015;116:600–611. doi: 10.1161/CIRCRESAHA.116.304899. [PubMed: 25563840]

19. Kaczmarek A, Vandenabeele P, Krysko DV. Necroptosis: the release of damage-associated molecular patterns and its physiological relevance. Immunity. 2013;38:209–223. [PubMed: 23438821]

20. Vanden Berghe T, Linkermann A, Jouan-Lanhouet S, Walczak H, Vandenabeele P. Regulated necrosis: the expanding network of non-apoptotic cell death pathways. Nat Rev Mol Cell Biol. 2014;15:135–147. [PubMed: 24452471]

21. Newton K, Dugger DL, Wickliffe KE, Kapoor N, de Almagro MC, Vucic D, Komuves L, Ferrando RE, French DM, Webster J, Roose-Girma M, Warming S, Dixit VM. Activity of protein kinase RIPK3 determines whether cells die by necroptosis or apoptosis. Science. 2014;343:1357–1360. [PubMed: 24557836]

22. Dondelinger Y, Declercq W, Montessuit S, Roelandt R, Goncalves A, Bruggeman I, Hulpiau P, Weber K, Sehon CA, Marquis RW, Bertin J, Gough PJ, Savvides S, Martinou JC, Bertrand MJ, Vandenabeele P. MLKL compromises plasma membrane integrity by binding to phosphatidylinositol phosphates. Cell Rep. 2014;7:971–981. doi: 10.1016/j.celrep.2014.04.026. [PubMed: 24813885]

23. Galluzzi L, Kepp O, Kroemer G. MLKL regulates necrotic plasma membrane permeabilization. Cell Res. 2014;24:139–140. doi: 10.1038/cr.2014.8. [PubMed: 24418759]

24. Sun L, Wang H, Wang Z, He S, Chen S, Liao D, Wang L, Yan J, Liu W, Lei X, Wang X. Mixed lineage kinase domain-like protein mediates necrosis signaling downstream of RIP3 kinase. Cell. 2012;148:213–227. doi: 10.1016/j.cell.2011.11.031. [PubMed: 22265413]

25. Mao Y, Luo W, Zhang L, Wu W, Yuan L, Xu H, Song J, Fujiwara K, Abe JI, LeMaire SA, Wang XL, Shen YH. STING-IRF3 triggers endothelial inflammation in response to free fatty acid-induced mitochondrial damage in diet-induced obesity. Arterioscler Thromb Vasc Biol. 2017;37:920–929. doi: 10.1161/ATVBAHA.117.309017. [PubMed: 28302626]

26. Seo E, Kang H, Choi H, Choi W, Jun HS. Reactive oxygen species-induced changes in glucose and lipid metabolism contribute to the accumulation of cholesterol in the liver during aging. Aging Cell. 2019;18:e12895. doi: 10.1111/acel.12895.

27. Zhao Q, Wei Y, Pandol SJ, Li L, Habtezion A. Sting signaling promotes inflammation in experimental acute pancreatitis. Gastroenterology. 2018;154:1822–1835 e1822. doi: 10.1053/j.gastro.2018.01.065. [PubMed: 29425920]

28. Benmerzoug S, Rose S, Bounab B, Gosset D, Duneau L, Chenuet P, Mollet L, Le Bert M, Lambers C, Geleff S, Roth M, Fauconnier L, Sedda D, Carvalho C, Perche O, Laurenceau D, Ryffel B, Apetoh L, Kiziltunc A, Uslu H, Albez FS, Akgun M, Togbe D, Quesniaux VFJ. STING-dependent sensing of self-DNA drives silica-induced lung inflammation. Nat Commun. 2018;9:5226. doi: 10.1038/s41467-018-07425-1. [PubMed: 30523277]

29. King KR, Aguirre AD, Ye YX, Sun Y, Roh JD, Ng RP, Jr., Kohler RH, Arlauckas SP, Iwamoto Y, Savol A, Sadreyev RI, Kelly M, Fitzgibbons TP, Fitzgerald KA, Mitchison T, Libby P, Nahrendorf M, Weissleder R. IRF3 and type I interferons fuel a fatal response to myocardial infarction. Nat Med. 2017;23:1481–1487. doi: 10.1038/nm.4428. [PubMed: 29106401]

30. Longo GM, Xiong W, Greiner TC, Zhao Y, Fiotti N, Baxter BT. Matrix metalloproteinases 2 and 9 work in concert to produce aortic aneurysms. J Clin Invest. 2002;110:625–632. doi: 10.1172/JCI15334. [PubMed: 12208863]

31. Jansen MP, Emal D, Teske GJ, Dessing MC, Florquin S, Roelofs JJ. Release of extracellular DNA influences renal ischemia reperfusion injury by platelet activation and formation of neutrophil extracellular traps. Kidney Int. 2017;91:352–364. doi: 10.1016/j.kint.2016.08.006. [PubMed: 27692564]
32. Escalante CR, Nistal-Villan E, Shen L, Garcia-Sastre A, Aggarwal AK. Structure of IRF-3 bound to the PRDIII-I regulatory element of the human interferon-beta enhancer. Mol Cell. 2007;26:703–716. doi: 10.1016/j.molcel.2007.04.022. [PubMed: 17560375]
33. Ma Z, Jacobs SR, West JA, Stopford C, Zhang Z, Davis Z, Barber GN, Glaunsinger BA, Dittmer DP, Damania B. Modulation of the cGAS-STING DNA sensing pathway by gammaherpesviruses. Proc Natl Acad Sci U S A. 2015;112:E4306–4315. doi: 10.1073/pnas.1503831112. [PubMed: 26199418]
34. Bell J Amlexanox for the treatment of recurrent aphthous ulcers. Clin Drug Investig. 2005;25:555–566.
35. Murray B, Biagioni PA, Lamey PJ. The efficacy of amlexanox OraDisc on the prevention of recurrent minor aphthous ulceration. J Oral Pathol Med. 2006;35:117–122. doi: 10.1111/j.1600-0714.2006.00379.x. [PubMed: 16430743]
36. Reilly SM, Chiang SH, Decker SJ, Chang L, Uhm M, Larsen MJ, Rubin JR, Mowers J, White NM, Hochberg I, Downes M, Yu RT, Liddle C, Evans RM, Oh D, Li P, Olefsky JM, Saltiel AR. An inhibitor of the protein kinases TBK1 and IKK-varepsilon improves obesity-related metabolic dysfunctions in mice. Nat Med. 2013;19:313–321. doi: 10.1038/nm.3082. [PubMed: 23396211]
37. Brault M, Olsen TM, Martinez J, Stetson DB, Oberst A. Intracellular nucleic acid sensing triggers necroptosis through synergistic type I IFN and TNF signaling. J Immunol. 2018;200:2748–2756. doi: 10.4049/jimmunol.1701492. [PubMed: 29540580]
38. Sarhan J, Liu BC, Muendlein HI, Weindel CG, Smirnova I, Tang AY, Ilyukha V, Sorokin M, Buzdin A, Fitzgerald KA, Poltorak A. Constitutive interferon signaling maintains critical threshold of MLKL expression to license necroptosis. Cell Death Differ. 2019;26:332–347. doi: 10.1038/s41418-018-0122-7. [PubMed: 29786074]
39. Ahn J, Barber GN. Self-DNA, STING-dependent signaling and the origins of autoinflammatory disease. Curr Opin Immunol. 2014;31:121–126. doi: 10.1016/j.coi.2014.10.009. [PubMed: 25459004]
40. West AP, Khoury-Hanold W, Staron M, Tal MC, Pineda CM, Lang SM, Bestwick M, Duguay BA, Raimundo N, MacDuff DA, Kaech SM, Smiley JR, Means RE, Iwasaki A, Shadel GS. Mitochondrial DNA stress primes the antiviral innate immune response. Nature. 2015;520:553–557. doi: 10.1038/nature14156. [PubMed: 25642965]
41. White MJ, McArthur K, Metcalf D, Lane RM, Cambier JC, Herold MJ, van Delft MF, Bedoui S, Lessene G, Ritchie ME, Huang DC, Kile BT. Apoptotic caspases suppress mtDNA-induced STING-mediated type I IFN production. Cell. 2014;159:1549–1562. doi: 10.1016/j.cell.2014.11.036. [PubMed: 25525874]
42. Kessler K, Borges LF, Ho-Tin-Noe B, Jondeau G, Michel JB, Vranckx R. Angiogenesis and remodelling in human thoracic aortic aneurysms. Cardiovasc Res. 2014;104:147–159. doi: 10.1093/cvr/cvu196. [PubMed: 25139748]
43. Michel JB, Jondeau G, Milewicz DM. From genetics to response to injury: vascular smooth muscle cells in aneurysms and dissections of the ascending aorta. Cardiovasc Res. 2018;114:578–589. doi: 10.1093/cvr/cvy006. [PubMed: 29360940]
44. Borissoff JI, Joosen IA, Versteylen MO, Brill A, Fuchs TA, Savchenko AS, Gallant M, Martinod K, Ten Cate H, Hofstra L, Crijns HJ, Wagner DD, Kietselaer B. Elevated levels of circulating DNA and chromatin are independently associated with severe coronary atherosclerosis and a prothrombotic state. Arterioscler Thromb Vasc Biol. 2013;33:2032–2040. doi: 10.1161/ATVBAHA.113.301627. [PubMed: 23818485]
45. Lehmann-Werman R, Neiman D, Zemmour H, Moss J, Magenheim J, Vaknin-Dembinsky A, Rubertsson S, Nellgard B, Blennow K, Zetterberg H, Spalding K, Haller MJ, Wasserfall CH, Schatz DA, Greenbaum CJ, Dorrell C, Grompe M, Zick A, Hubert A, Maoz M, Fendrich V, Bartsch DK, Golan T, Ben Sasson SA, Zamir G, Razin A, Cedar H, Shapiro AM, Glaser B, Shemer R, Dor Y. Identification of tissue-specific cell death using methylation patterns of

circulating DNA. Proc Natl Acad Sci U S A. 2016;113:E1826–1834. doi: 10.1073/pnas.1519286113. [PubMed: 26976580]

46. Rumore PM, Steinman CR. Endogenous circulating DNA in systemic lupus erythematosus. Occurrence as multimeric complexes bound to histone. J Clin Invest. 1990;86:69–74. doi: 10.1172/JCI114716. [PubMed: 2365827]
47. Imokawa S, Satou A, Taniguchi M, Toyoshima M, Nakazawa K, Hayakawa H, Chida K. [Amlexanox has an acute bronchodilator effect in patients with aspirin-induced asthma (AIA)]. Nihon Kyobu Shikkan Gakkai Zasshi. 1993;31:976–982. [PubMed: 8230896]
48. Reilly SM, Ahmadian M, Zamarron BF, Chang L, Uhm M, Poirier B, Peng X, Krause DM, Korytnaya E, Neidert A, Liddle C, Yu RT, Lumeng CN, Oral EA, Downes M, Evans RM, Saltiel AR. A subcutaneous adipose tissue-liver signalling axis controls hepatic gluconeogenesis. Nat Commun. 2015;6:6047. doi: 10.1038/ncomms7047. [PubMed: 25581158]
49. Yu J, Zhou X, Chang M, Nakaya M, Chang JH, Xiao Y, Lindsey JW, Dorta-Estremera S, Cao W, Zal A, Zal T, Sun SC. Regulation of T-cell activation and migration by the kinase TBK1 during neuroinflammation. Nat Commun. 2015;6:6074. doi: 10.1038/ncomms7074. [PubMed: 25606824]
50. Wang XA, Zhang R, She ZG, Zhang XF, Jiang DS, Wang T, Gao L, Deng W, Zhang SM, Zhu LH, Guo S, Chen K, Zhang XD, Liu DP, Li H. Interferon regulatory factor 3 constrains IKKbeta/NF-kappaB signaling to alleviate hepatic steatosis and insulin resistance. Hepatology. 2014;59:870–885. doi: 10.1002/hep.26751. [PubMed: 24123166]

Clinical Perspective

What is New?

- DNA damage and activation of cytosolic DNA sensing adaptor STING signaling are significantly increased in aortic tissues from patients with sporadic thoracic aortic aneurysm and dissection.
- By promoting smooth muscle cell (SMC) death and mediating SMC death-induced macrophage activation and MMP production, cytosolic DNA and cytosolic DNA sensing adaptor STING signaling play a critical role in aortic destruction and aortic disease development.
- Single-cell transcriptome analysis of aortic tissues from wild-type and *Sting*-deficient mice comprehensively reveals dynamic SMC and macrophage populations and differentially expressed gene profiles after aortic challenge.

What are the Clinical Implications?

- Cytosolic DNA and abnormal activation of cytosolic DNA sensing signaling play critical roles in sporadic aortic destruction, dilatation, dissection, and rupture.
- Targeting the cytosolic DNA sensing adaptor STING pathway may block the vicious cycle of aortic cell injury and inflammation and prevent aortic aneurysm and dissection formation and progression.

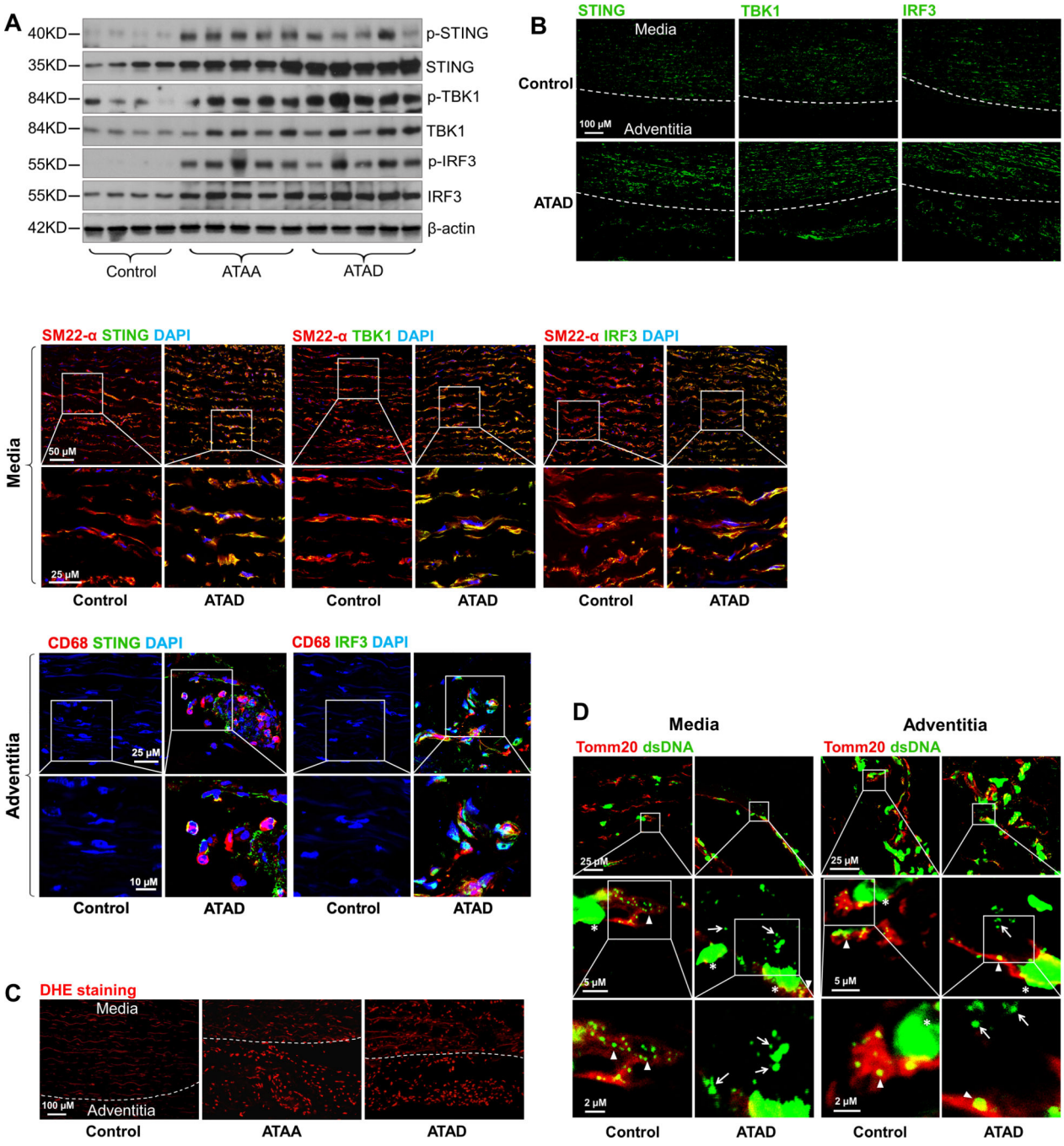

Figure 1. Presence of cytosolic DNA and activation of the STING signaling pathway in human sporadic ascending thoracic aortic aneurysm and dissection (ATAAD) tissues.

Aortic tissues from patients with ascending thoracic aortic aneurysm (ATAA) (n=10), patients with acute ascending thoracic aortic dissection (ATAD) (n=10), and organ donors (control) (n=8) were analyzed. **A**, Representative western blot data showing that the STING pathway was activated in the aortic wall of ATAAD patients. **B**, Immunostaining showing that the levels of STING, TBK1, and IRF3 were increased in diseased aortas, particularly in smooth muscle cells (SM22-α) and macrophages (CD68). Insets show a higher

magnification view. **C**, Representative images of dihydroethidium (DHE) staining showing increased reactive oxygen species production in the aortic wall of ATAAD patients. **D**, Representative immunostaining of DNA and mitochondria (Tomm20) showing cytosolic DNA (not located in nuclei or mitochondria) in smooth muscle cells of the aortic media and in macrophages of the adventitia in ATAD tissues. Insets show a higher magnification view. Asterisk indicates nuclear DNA (nDNA). Arrowhead indicates mitochondrial DNA (mtDNA). Arrow indicates cytosolic DNA (ctDNA).

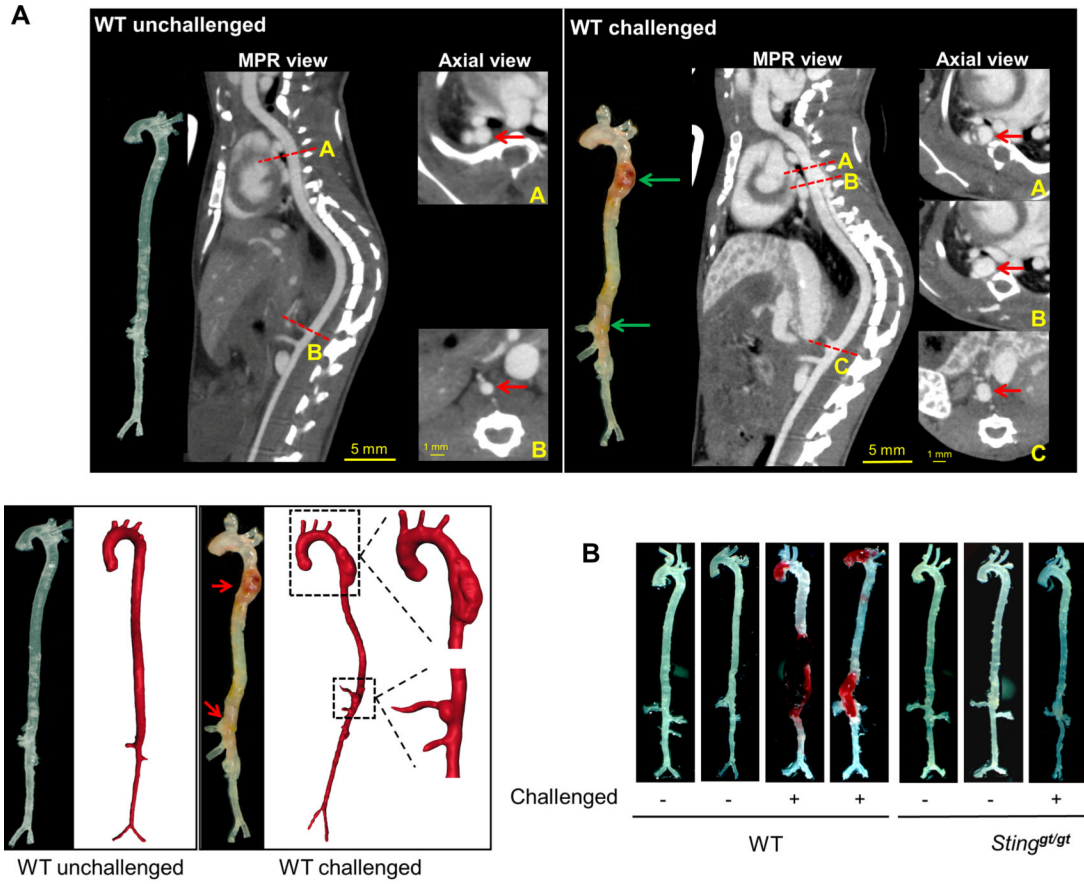

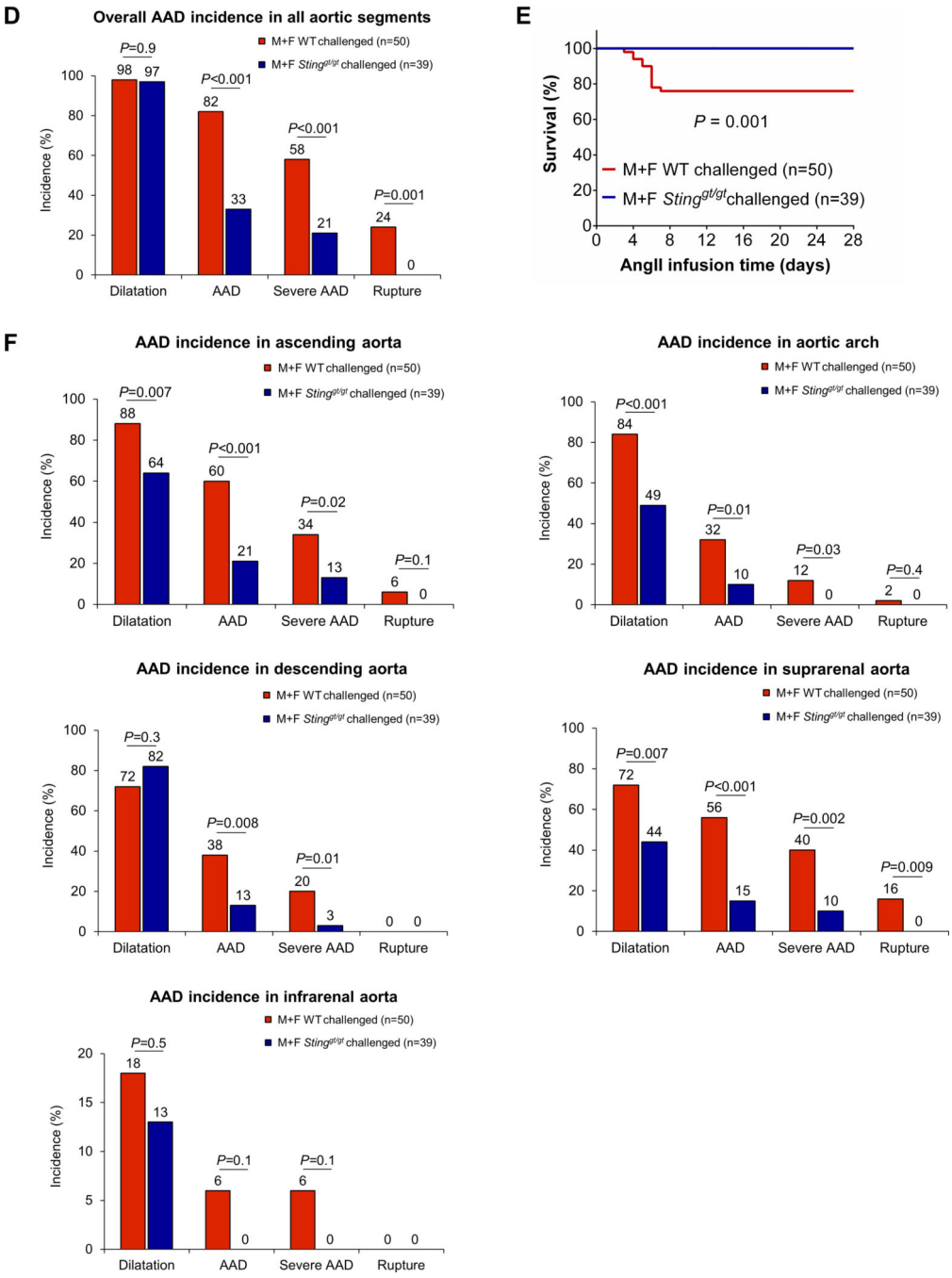

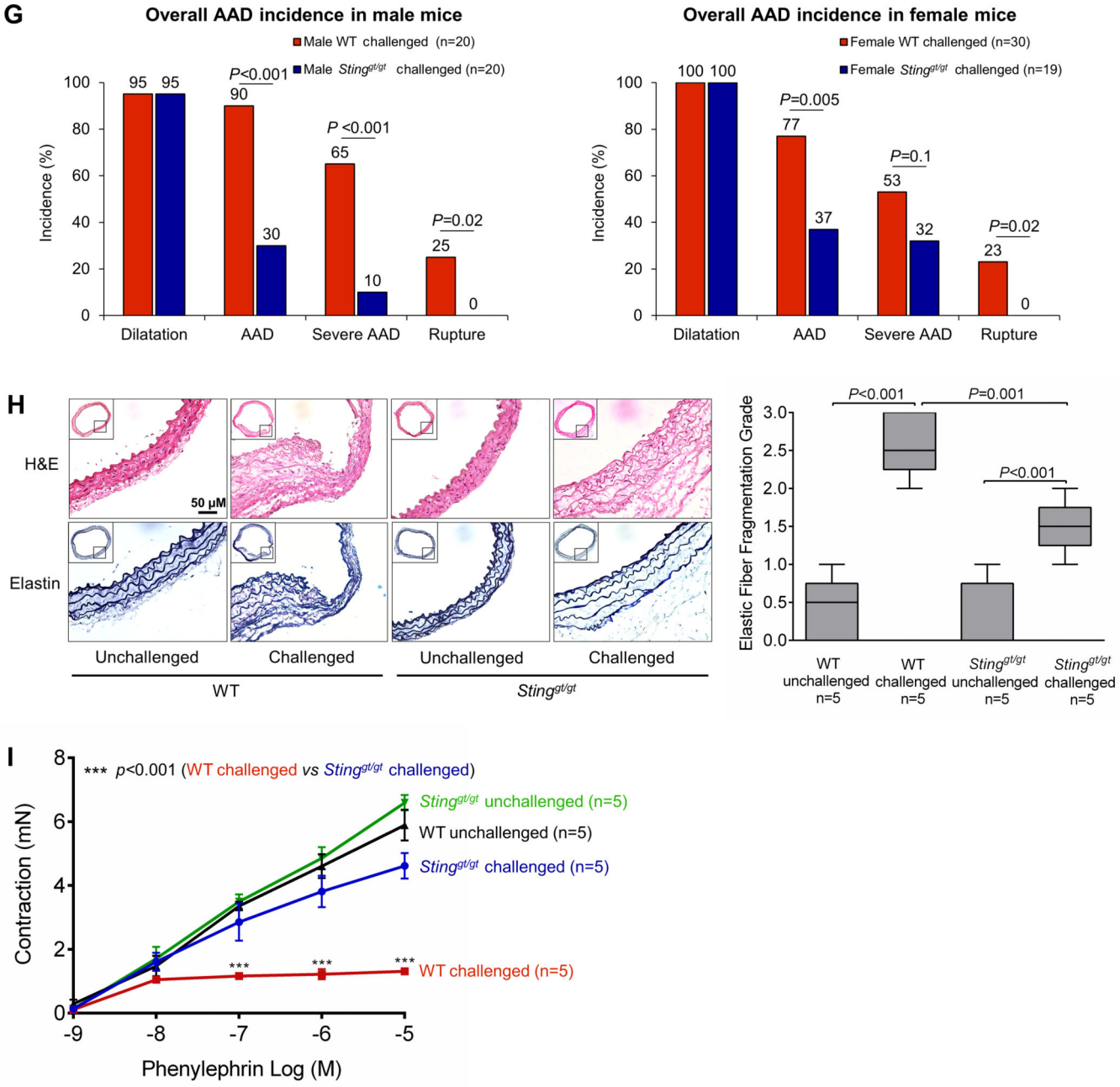

Figure 2. Reduced incidence of aortic aneurysm and dissection (AAD) and preserved aortic structure and contractile ability in challenged *Sting*-deficient (*Sting*$^{gt/gt}$) mice.

Wild-type (WT) mice and *Sting*$^{gt/gt}$ mice were unchallenged or challenged with a high-fat diet for 8 weeks and angiotensin II infusion (2000 ng/min/kg) during the last 4 weeks. **A**, Representative computed tomography angiography (CTA) images of aortas from challenged WT mice showing the presence of AAD in the thoracic and suprarenal aortic segments. **B**, Representative images of excised aortas showing less aortic damage in challenged *Sting*$^{gt/gt}$ mice than in challenged WT mice. **C**, Mean aortic diameters of various aortic segments were smaller in challenged *Sting*$^{gt/gt}$ mice than in challenged WT mice. The measurements were based on the excised aortas (as shown in B). Asc, ascending; Desc, descending; SR,

suprarenal; IR, infrarenal. **D**, The overall incidences of AAD, severe AAD, and rupture were significantly lower in challenged *Sting*$^{gt/gt}$ mice than in challenged WT mice. **E**, Kaplan-Meier survival analysis showing improved survival in challenged *Sting*$^{gt/gt}$ mice compared with challenged WT mice during the 4 weeks of angiotensin II infusion. **F**, The incidence of AAD in different aortic segments was significantly lower in challenged *Sting*$^{gt/gt}$ mice than in challenged WT mice. **G**, The lower overall AAD incidence in challenged *Sting*$^{gt/gt}$ mice was similar in male and female mice. **H**, Representative hematoxylin and eosin (H&E) staining and Verhoeff–van Gieson elastin staining (elastin) of ascending aortic sections showing preserved aortic structure in *Sting*$^{gt/gt}$ mice compared with challenged WT mice. The quantification of aortic elastic fiber fragmentation showing less aortic destruction in challenged *Sting*$^{gt/gt}$ mice than in challenged WT mice. **I**, Wire myograph analysis of ascending thoracic aortic rings showing a significantly reduced contractile response to phenylephrine in challenged WT mice compared with unchallenged WT mice. Challenged *Sting*$^{gt/gt}$ mice exhibited partial preservation of contractile ability. Two-way ANOVA with the Bonferroni post-hoc test was used for pairwise comparisons in **(C)** and **(H).** The Fisher exact test was used for **(D)**, **(F)**, and **(G)**. Multi-way analysis of variance with the Holm-Šídák test was used for pairwise comparisons in **(I).** ***P<0.001. Data are presented as the mean ± standard error of the mean.

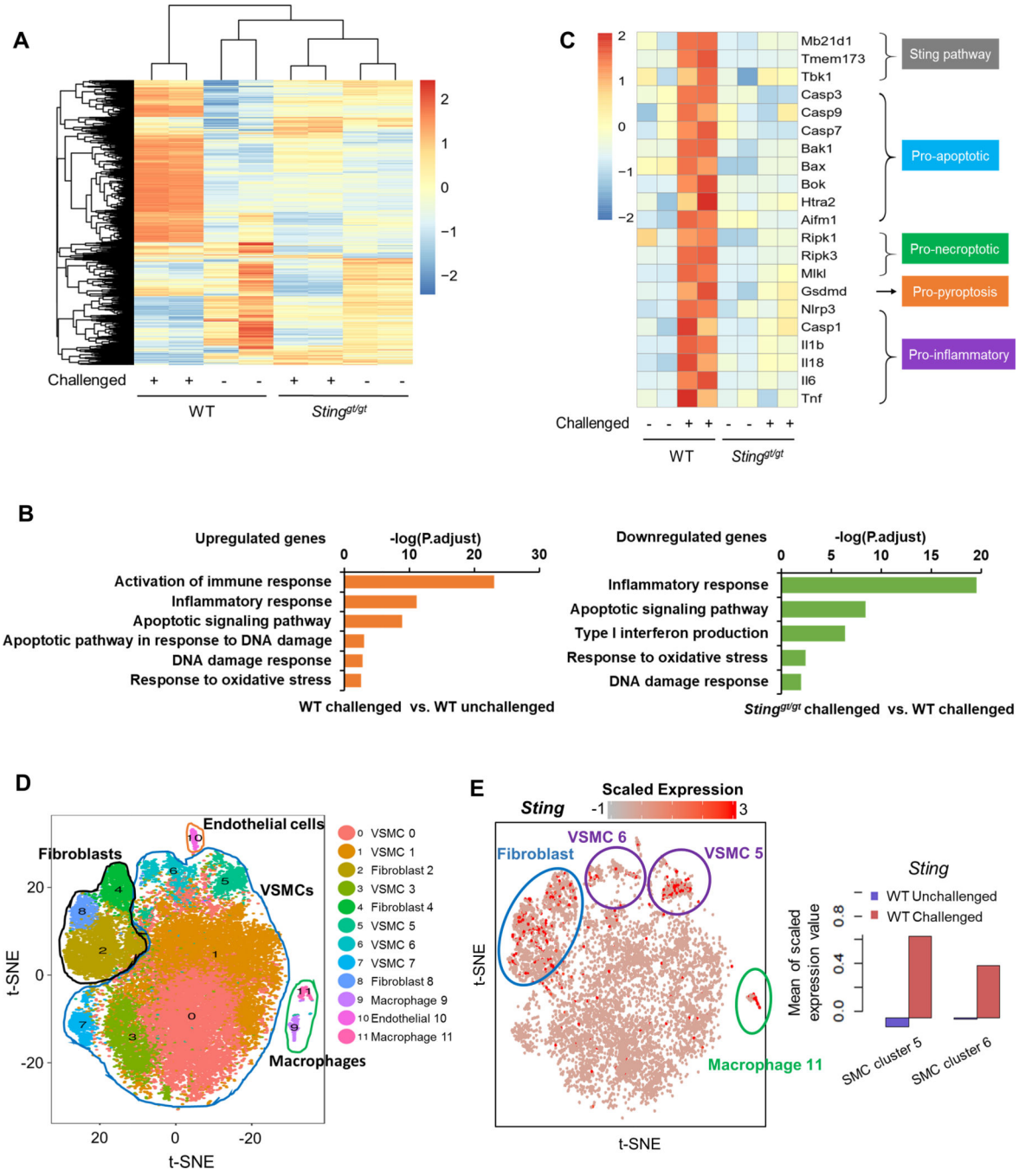

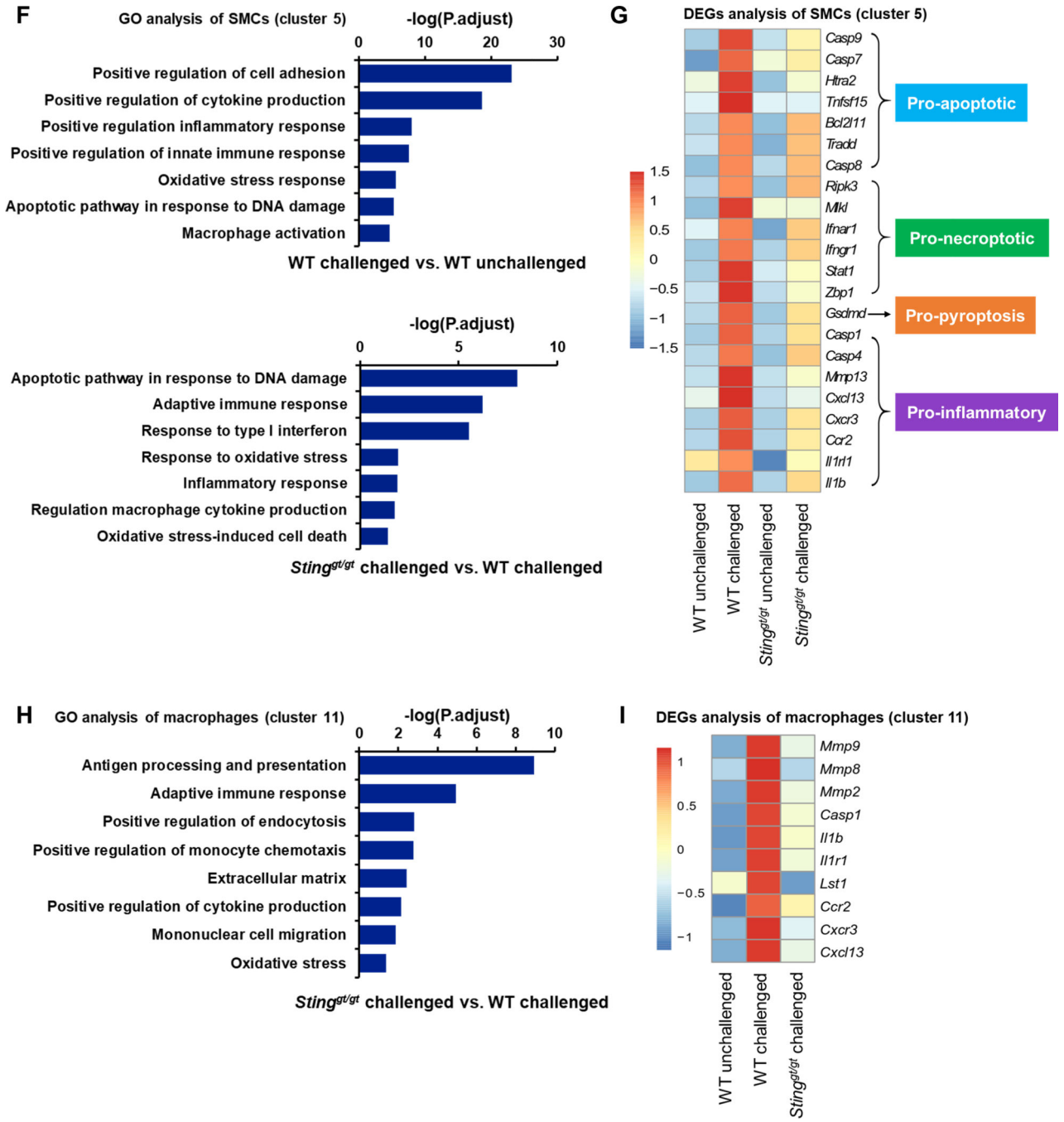

Figure 3. Prevention of the aortic challenge–induced expression of genes involved in smooth muscle cell (SMC) death and inflammation in *Sting*$^{gt/gt}$ mice.

A-C, Bulk RNA-sequencing (RNA-seq) analysis was performed in ascending aortas from wild-type (WT) mice and *Sting*$^{gt/gt}$ mice that were unchallenged or challenged with a high-fat diet (HFD) for 5 weeks and angiotensin II (AngII; 2000 ng/min/kg) infusion during the last week. For each group, 5 aortas were pooled as 1 sample, and duplicate samples were tested. **A**, Heatmap showing different gene expression patterns among groups. **B**, Gene ontology (GO) analysis showing that aortic challenge induced the expression of genes

involved in several biologic processes (left) and that this induction was prevented in *Sting*$^{gt/gt}$ mice (right). **C**, Heatmap showing that *Sting* deficiency prevented the challenge-induced upregulation of genes involved in the STING pathway, cell death pathways (apoptosis, necroptosis, and pyroptosis), and the inflammatory response **D-I**, Single-cell transcriptome analysis was performed in ascending aortas from WT mice and *Sting*$^{gt/gt}$ mice that were unchallenged or challenged with a HFD for 5 weeks AngII (2000 ng/min/kg) infusion during the last week. For each group, single cell suspensions from 3 aortas were pooled as one sample. VSMC, vascular smooth muscle cell. **D**, t-Stochastic neighbor embedding (t-SNE) plots from the ascending aortas of WT mice showing 12 different cell clusters, including 6 clusters of SMCs and 2 clusters of macrophages. **E**, *Sting* expression was projected onto t-SNE plots of challenged WT mice showing the high expression of *Sting* in SMCs, macrophages, and fibroblasts (left). Quantification showing that aortic challenge increased *Sting* gene expression in SMC cluster 5 and SMC cluster 6 (right). **F**, GO enrichment analysis of *Sting*-positive SMCs (cluster 5) showing that aortic challenge induced the expression of several genes with roles in different biologic processes (up) but that this was prevented in challenged *Sting*- deficient mice (down). **G**, Heatmap of *Sting*-positive SMCs (cluster 5) showing that *Sting* deficiency prevented the challenge-induced expression of genes in inflammation and cell death (apoptosis, necroptosis, and pyroptosis). **H**, GO enrichment analysis of *Sting*-positive macrophages (cluster 11) showing that *Sting* deficiency prevented the aortic challenge-induced expression of several genes. **I**, Heatmap of *Sting*-positive macrophages (cluster 11) showing that *Sting* deficiency prevented the challenge-induced upregulation of genes involved in inflammation.

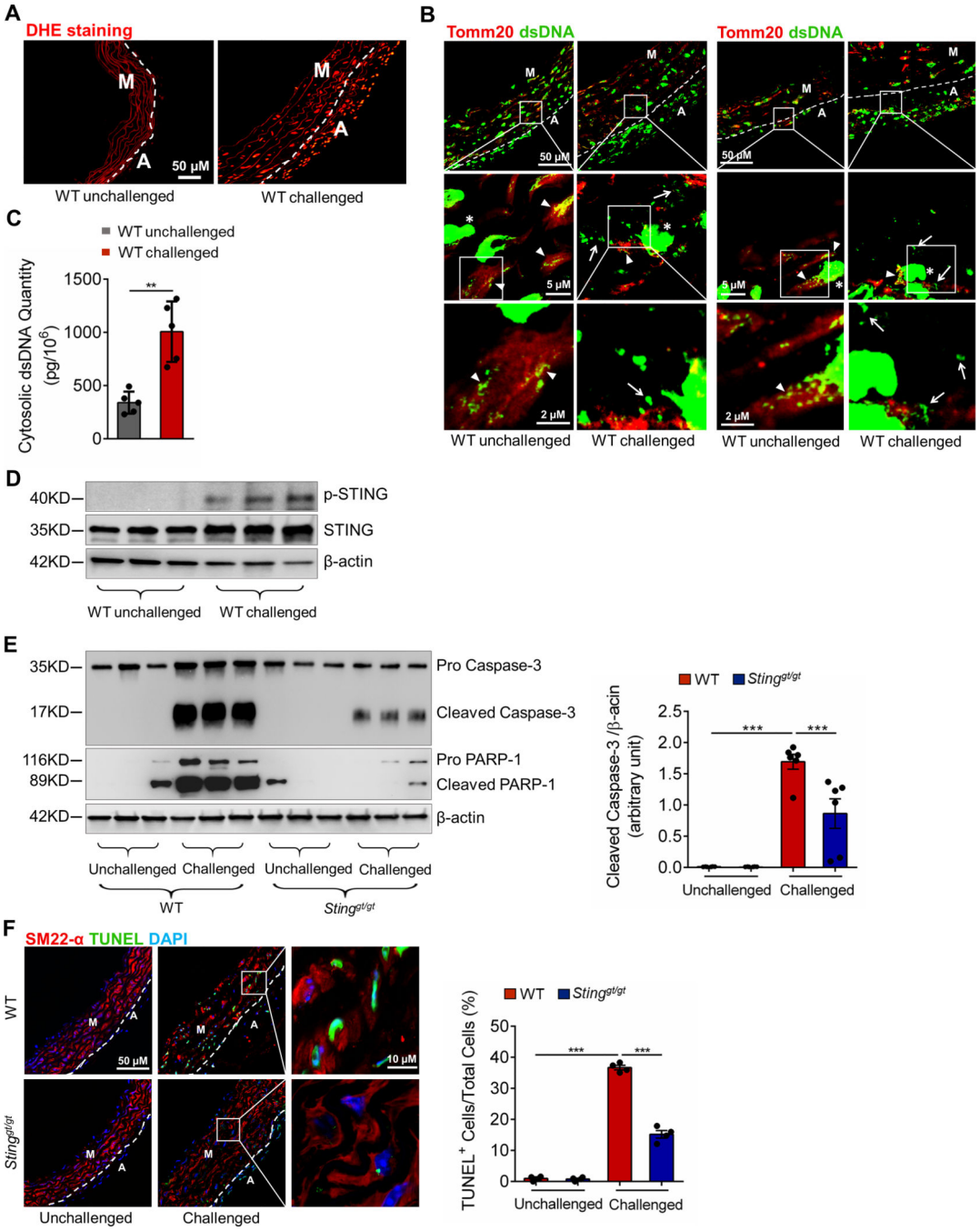

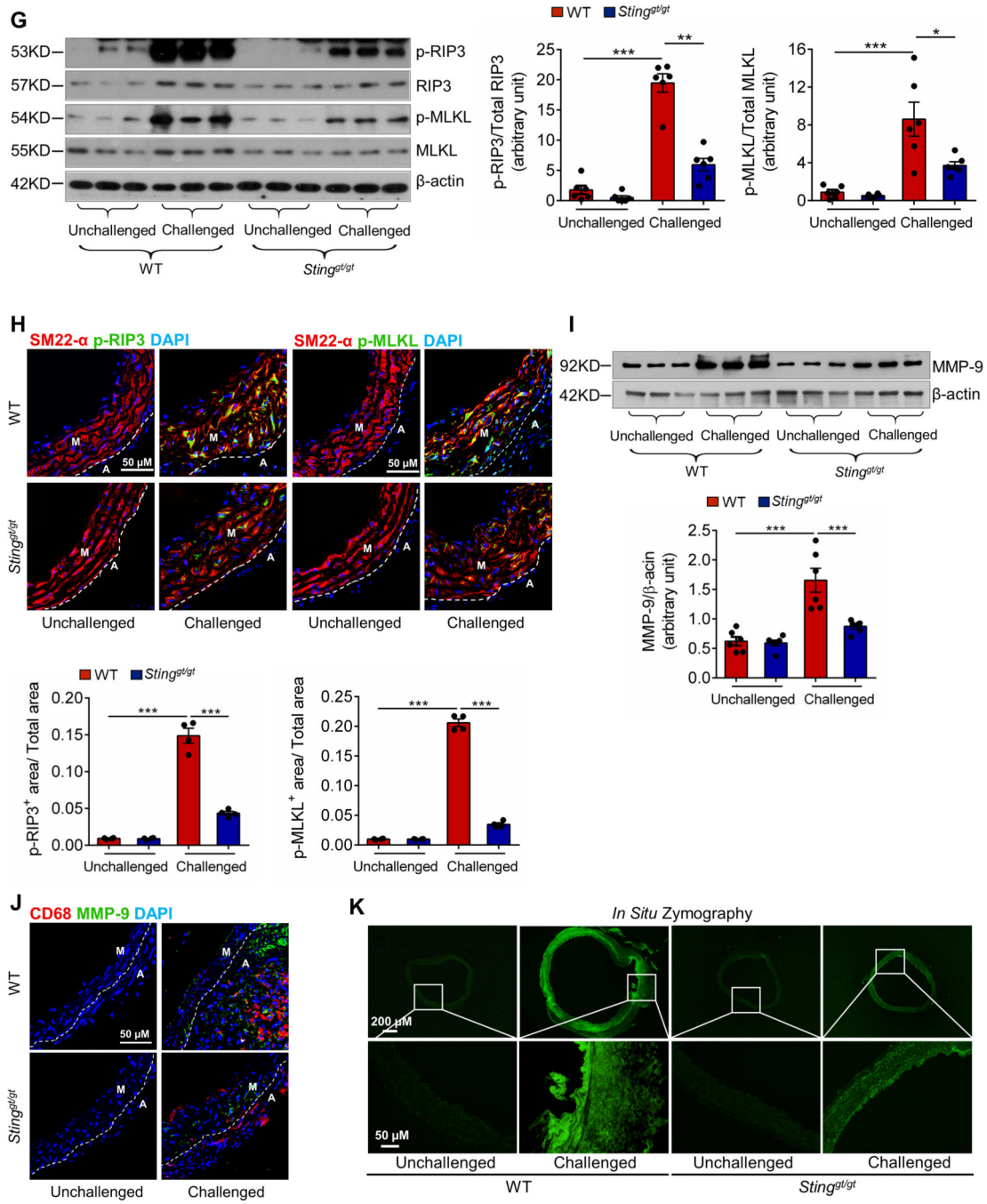

Figure 4. Prevention of challenge-induced smooth muscle cell (SMC) death and macrophage MMP-9 production in *Sting*-deficient (*Sting*$^{gt/gt}$) mice.

Analyses were performed by using ascending aortas from wild-type (WT) mice and *Sting*$^{gt/gt}$ mice that were unchallenged or challenged with a high-fat diet for 8 weeks and angiotensin II infusion (2000 ng/min/kg) during the last 4 weeks. **A**, Representative images of dihydroethidium (DHE) staining showing increased reactive oxygen species production in the aortic wall (M, media; A, adventitia) of challenged wild-type (WT) mice. **B**, Representative immunostaining of DNA and mitochondria (Tomm20) showing cytosolic

DNA in SMCs of the aortic media and in macrophages of the adventitia in challenged WT mice (M: media; A: adventitia). Insets show a higher-magnification view. Asterisk indicates nuclear DNA. Arrowhead indicates mitochondrial DNA. Arrow indicates cytosolic DNA. **C**, Bar graph showing that the quantity of cytosolic double-stranded DNA (dsDNA) was increased in aortic cells of the ascending aorta of challenged WT mice compared with unchallenged WT mice (n=5 per group). **D**, Western blot analysis showing that aortic challenge in WT mice induced a marked increase in the levels of phosphorylated STING in the ascending aorta (n=3 per group). **E**, Western blot analysis and quantification data showing that the cleavage of caspase-3 and PARP-1 was reduced in ascending aortas from challenged *Sting*$^{gt/gt}$ mice compared with those from challenged WT mice (n=6 per group). **F**, Representative terminal deoxynucleotidyl transferase dUTP nick end labeling (TUNEL)-stained images and quantification data showing that the number of apoptotic aortic SMCs was reduced in challenged *Sting*$^{gt/gt}$ mice compared with challenged WT mice (n=4 per group) (M: media; A: adventitia). **G**, Western blot analysis and quantification data showing that the phosphorylation of RIP3 (p-RIP3) and MLKL (p-MLKL) in the ascending aorta was reduced in challenged *Sting*$^{gt/gt}$ mice compared with challenged WT mice (n=6 per group). **H**, Representative immunofluorescence staining and quantification data showing that the levels of p-RIP3 and p-MLKL in aortic SMCs (SM22-α) were reduced in challenged *Sting*$^{gt/gt}$ mice compared with challenged WT mice (n=4 per group) (M: media; A: adventitia). **I**, Western blot analysis and quantification showing that MMP-9 expression in the ascending aorta was reduced in challenged *Sting*$^{gt/gt}$ mice compared with challenged WT mice (n=6 per group). **J**, Representative immunofluorescence staining showing that MMP-9 expression in macrophages (CD68) was decreased in aortas from challenged *Sting*$^{gt/gt}$ mice compared with those from challenged WT mice (M: media; A: adventitia). **K**, *In situ* zymography results showing that MMP activity in the aorta was decreased in challenged *Sting*$^{gt/gt}$ mice compared with challenged WT mice. Insets show a higher magnification view. An unpaired two-tailed *t*-test was used in **(C)**. Two-way ANOVA with the Bonferroni post-hoc test was used for pairwise comparisons in **(E)** through **(I)**. *$P<0.05$, **$P<0.01$, ***$P<0.001$. Data are presented as the mean ± standard error of the mean.

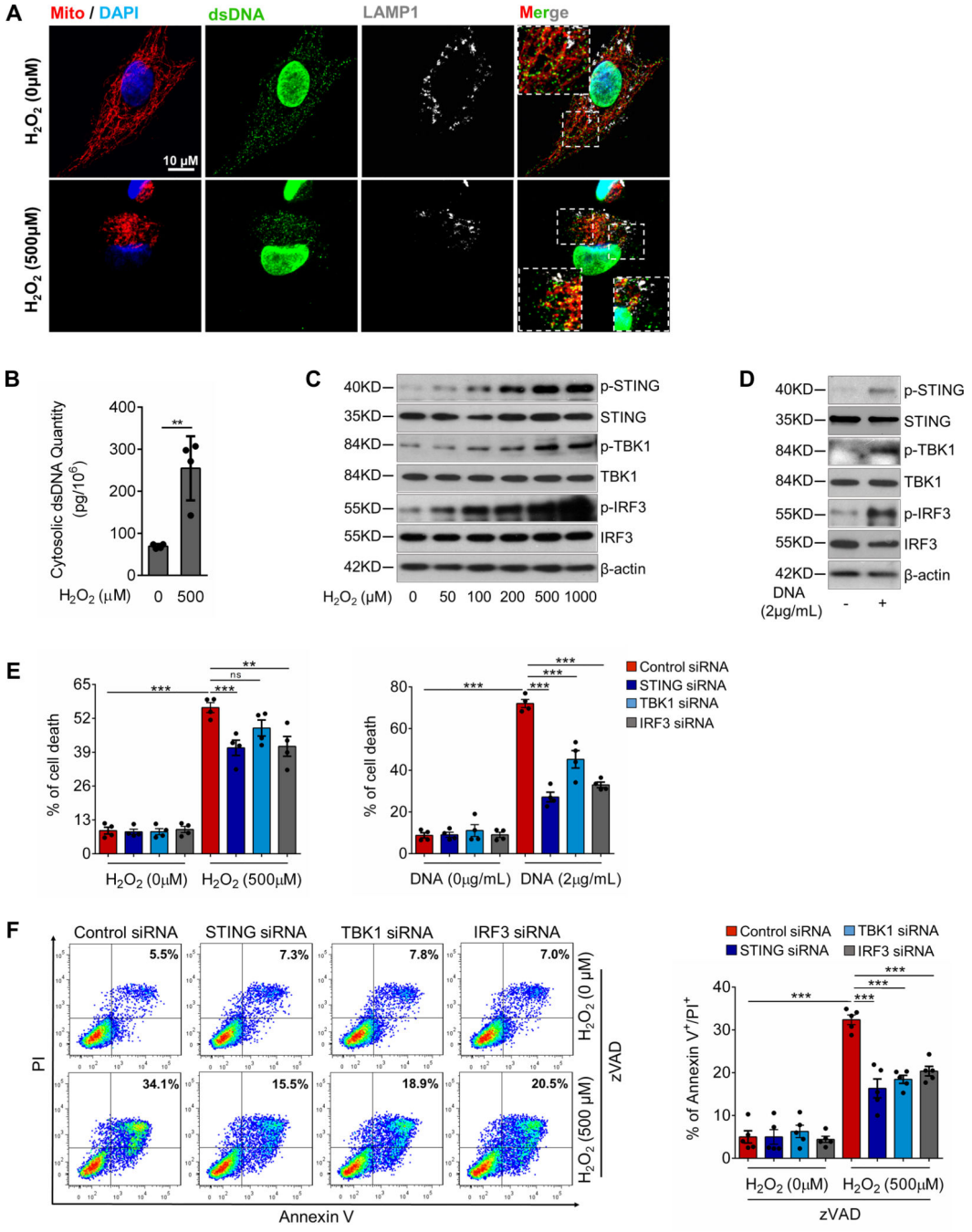

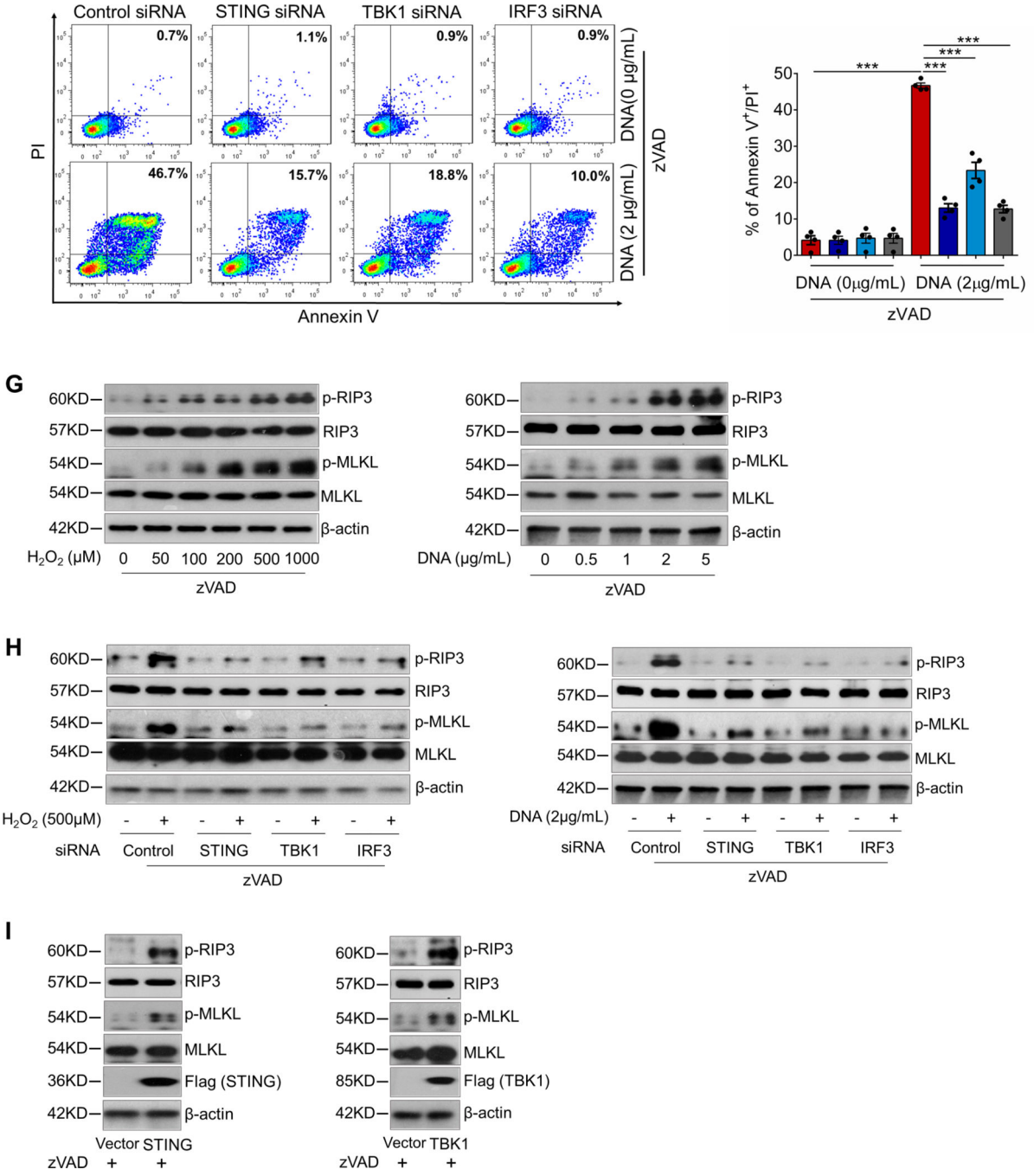

Figure 5. Critical role of the STING-TBK1-IRF3 pathway in aortic smooth muscle cell (SMC) injury.

A, Representative immunostaining of DNA, mitochondria (MitoTracker), and lysosomes (LAMP1) showing mitochondrial DNA (mtDNA; double-stranded DNA [dsDNA] that colocalized with MitoTracker), nuclear DNA (dsDNA in the nuclei), and cytosolic DNA (dsDNA that did not colocalize with either mitochondria, nuclei, or lysosomes) in cultured SMCs (n=5 biologic repeats). H_2O_2 treatment increased the amount of cytosolic DNA in SMCs. Insets show a higher magnification view. **B**, Bar graph showing that the

concentration of cytosolic dsDNA was increased in H_2O_2-treated SMCs compared with control SMCs (n=4 biologic repeats). **C**, Western blot analysis showing that H_2O_2 increased the phosphorylation of STING, TBK1, and IRF3 in SMCs in a dose-dependent manner. **D**, Western blot results showing that transfection with exogenous SMC DNA from H_2O_2-treated SMCs activated the STING pathway in SMCs. **E**, Flow cytometry analyses showing that silencing STING, TBK1, or IRF3 with siRNA partially prevented cell death induced by H_2O_2 or exogenous SMC DNA (n=4 biologic repeats). **F**, Flow cytometry analysis showing that silencing STING, TBK1, or IRF3 with siRNA prevented necroptotic cell death induced by H_2O_2 or exogenous SMC DNA (n=4 or 5 biologic repeats). PI, propidium iodide. **G**, Western blot analysis showing that H_2O_2 or exogenous SMC DNA induced the expression and phosphorylation of RIP3 and MLKL in a dose-dependent manner in SMCs pretreated with zVAD. **H**, Western blot results showing that silencing STING, TBK1, or IRF3 with siRNA prevented the H_2O_{2-} or exogenous SMC DNA–induced activation and phosphorylation of RIP3 and MLKL in SMCs pretreated with zVAD. **I**, Western blot results showing that the overexpression of STING or TBK1 increased the activation and phosphorylation of RIP3 and MLKL in SMCs pretreated with zVAD. An unpaired two-tailed *t*-test was used in **(B)**. Two-way ANOVA with Bonferroni's post-hoc test for pairwise comparisons was used in **(E)** and **(F)**. ns indicates not significant. $^{**}P<0.01$, $^{***}P<0.001$. Data are presented as the mean ± standard error of the mean.

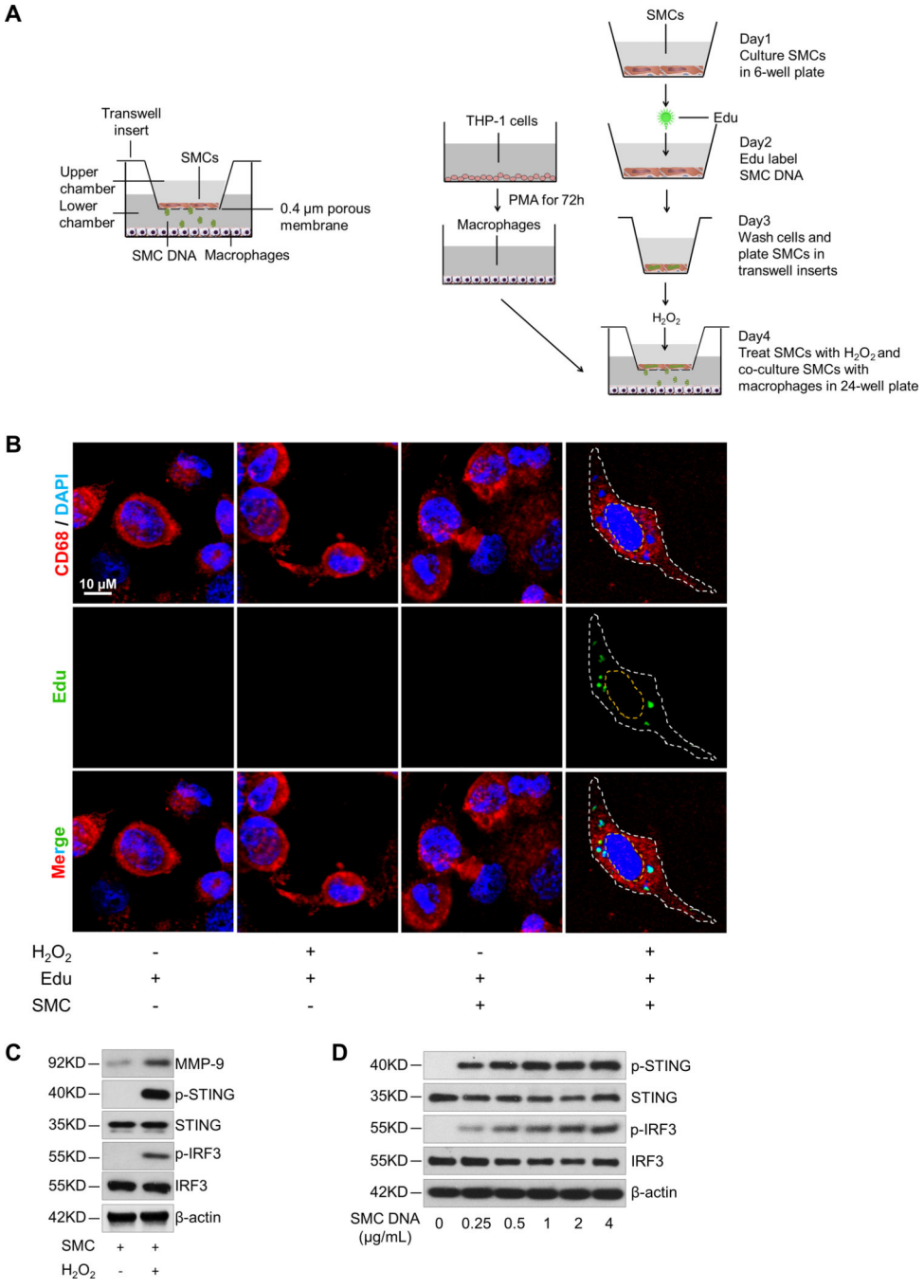

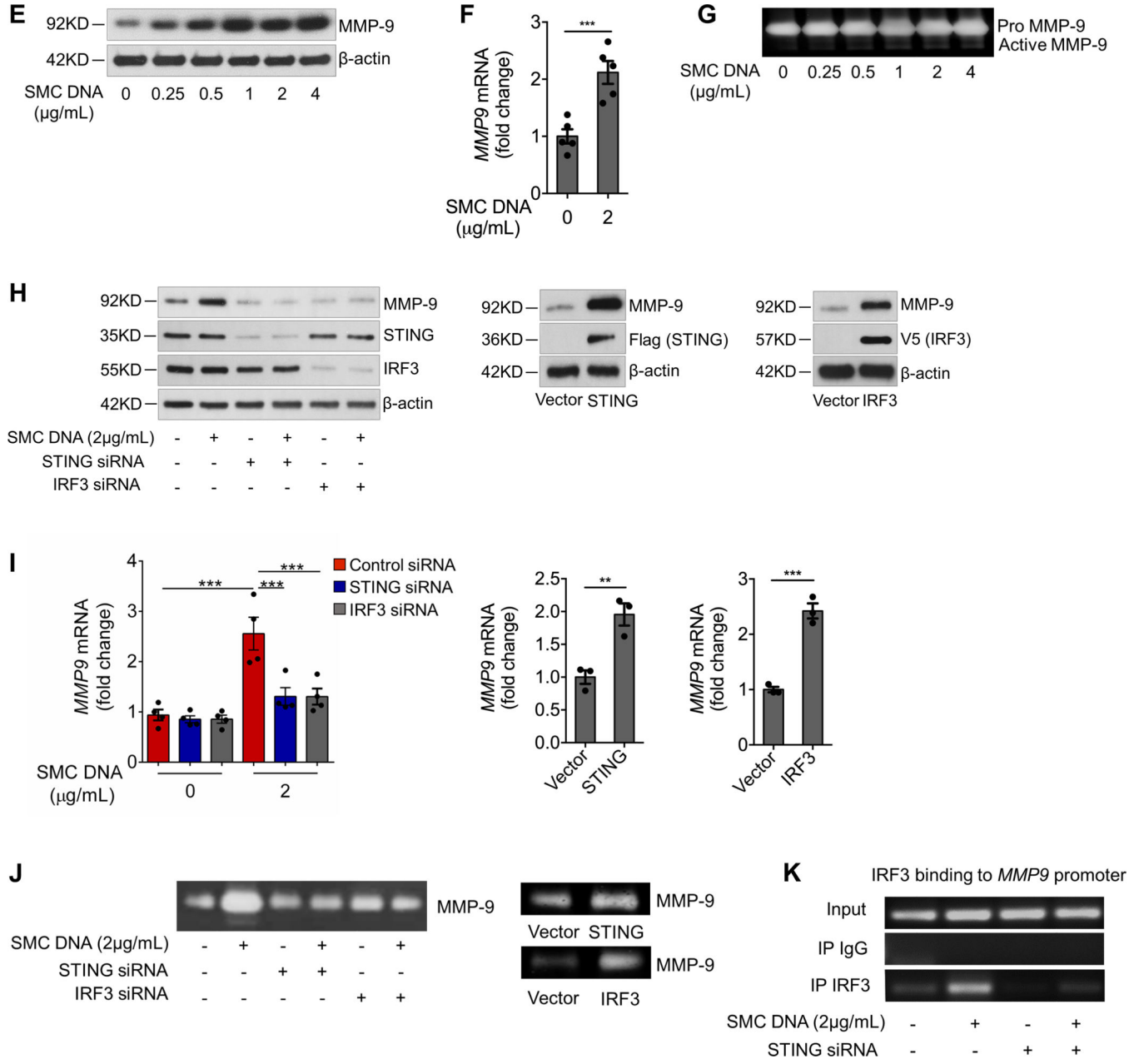

Figure 6. DNA from aortic smooth muscle cells (SMCs) induced MMP-9 production in macrophages through the STING pathway.

A, Illustration of the transwell co-culture system. The upper schematic shows that the transwell comprised a 24-well culture insert with a 0.4-μm pore size in the upper part and a 24-well plate in the lower part. The lower schematic shows the experimental procedure. PMA, phorbol 12-myristate 13-acetate. **B**, Immunofluorescence staining showing the presence of DNA from Edu-labeled H_2O_2-treated SMCs in the cytosol of macrophages (CD68) after using a transwell co-culture system. Cells are outlined with white dots. Nuclei are outlined with yellow dots. **C**, Western blot showing that MMP-9 expression and the phosphorylation of STING and IRF3 were increased in macrophages that were co-cultured with H_2O_2-treated SMCs. **D-G**, Macrophages were transfected with DNA isolated from

H_2O_2-treated SMCs. SMC-derived DNA increased the expression and phosphorylation of STING and IRF3. **(D)**, SMC-derived DNA also increased levels of MMP-9 protein **(E)**, *MMP9* mRNA **(F)**, and MMP-9 activity **(G)** (n=5 biologic repeats). **H-K,** Macrophages were transfected with STING or IRF3 plasmid DNA or transfected with STING or IRF3 siRNA, followed by stimulation with SMC DNA. MMP-9 protein levels (n=4 biologic repeats) **(H)**, *MMP9* mRNA levels (n=3 biologic repeats) **(I)**, and MMP-9 activity **(J)** were enhanced by the overexpression of STING or IRF3 or reduced by the knockdown of *STING* or *IRF3*. **K**, The results of a chromatin immunoprecipitation assay showing that IRF3 bound to the *MMP9* promoter in unstressed macrophages. This binding was increased in cells treated with SMC DNA and was abolished by inhibiting STING expression with STING siRNA (n=4 biologic repeats). An unpaired, two-tailed *t*-test was used in **(F)** and **(I)**. Two-way ANOVA with the Bonferroni post-hoc test for pairwise comparisons was used in **(I)**. $^{**}P<0.01$, $^{***}P<0.001$. Data are presented as the mean ± standard error of the mean.

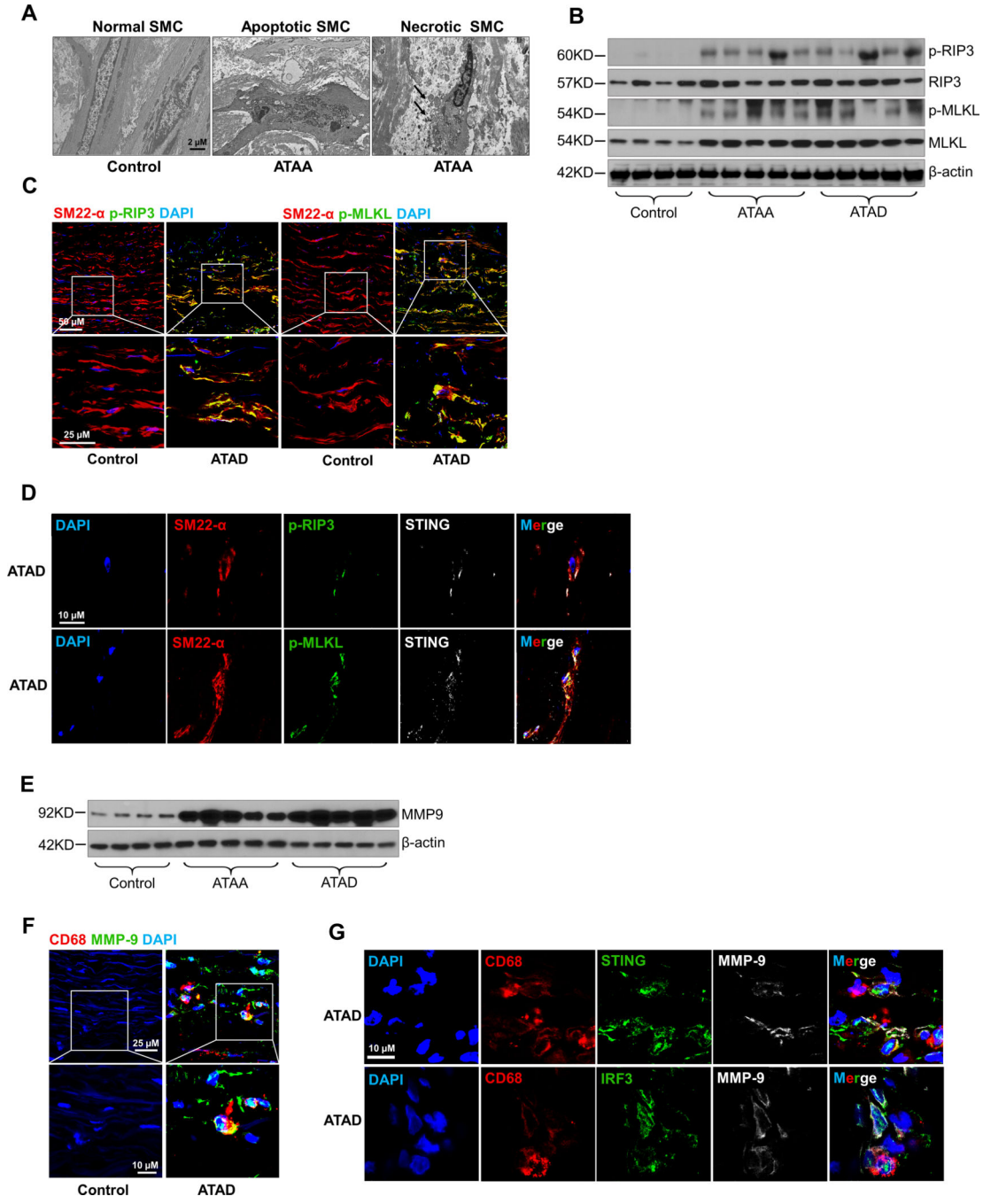

Figure 7. Association of STING activation with smooth muscle cell (SMC) injury and MMP-9 production in human sporadic ascending thoracic aortic aneurysm and dissection (ATAAD) tissues.

A, Electron microscopy images of ascending thoracic aortic aneurysm (ATAA) patient tissue showing apoptotic SMC death with nuclear fragmentation, chromatin condensation, and blebbing of the cell membrane and necrotic SMC death with swollen nuclei, mitochondria, and endoplasmic reticulum. **B**, Western blot analysis showing increased phosphorylation of RIP3 (p-RIP3) and MLKL (p-MLKL) in the aortic wall of ATAAD patients. **C**, Immunostaining showing increased p-RIP3 and p-MLKL levels in SMCs (SM22-α) of

ascending thoracic aortic dissection (ATAD) tissues. Insets show a higher-magnification view. **D**, Immunostaining showing the colocalization of STING with p-RIP3 and p-MLKL in the SMCs (SM22-α) of ATAD tissues. **E**, Western blot analysis showing increased MMP-9 levels in ATAAD patient tissues. **F**, Immunostaining showing increased MMP-9 expression in macrophages (CD68) of diseased tissues from patients with ATAD and **G,** the colocalization of MMP-9 with STING and IRF3 in macrophages (CD68) of diseased tissues from patients with ATAD. Insets show a higher-magnification view.

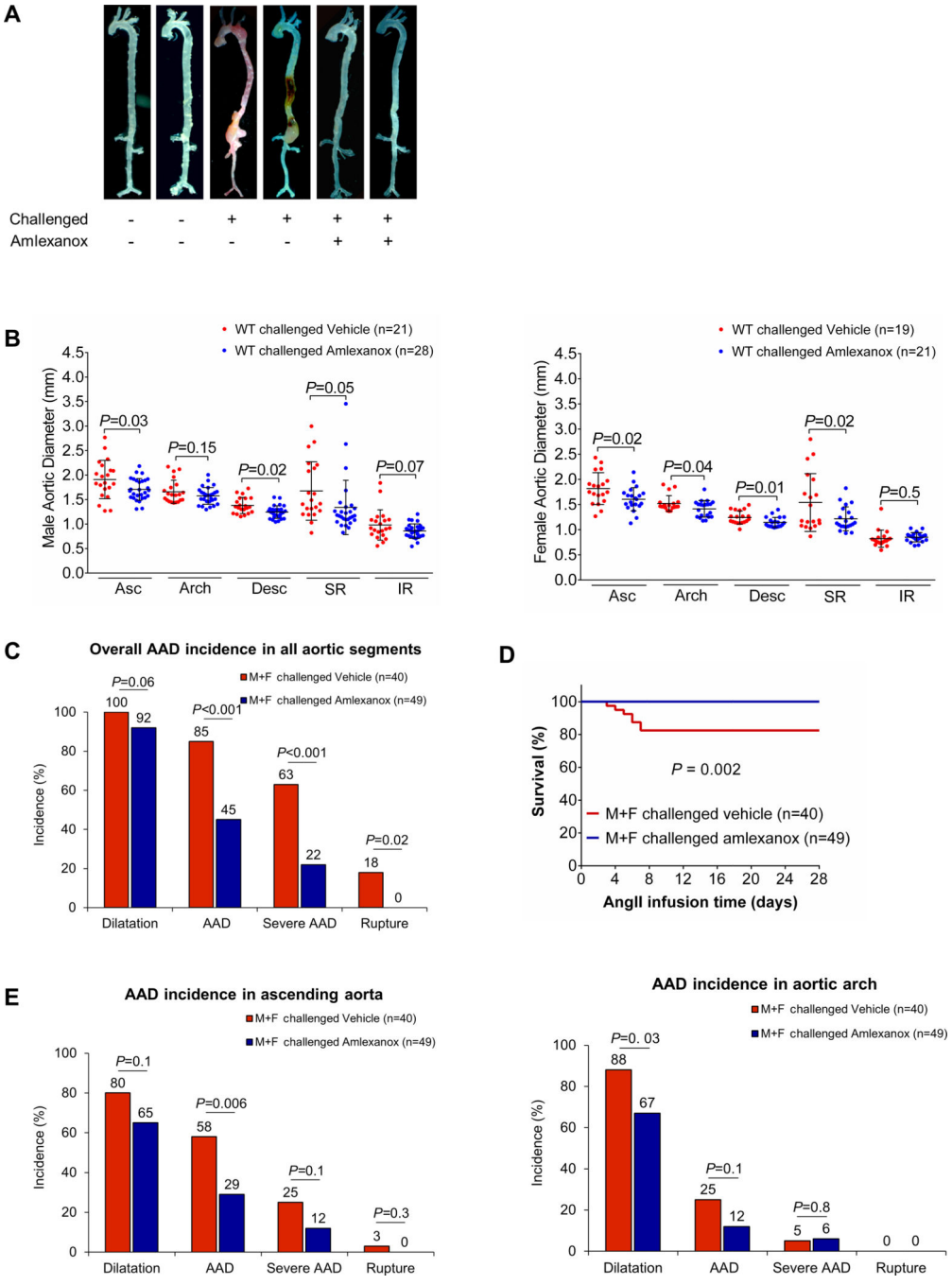

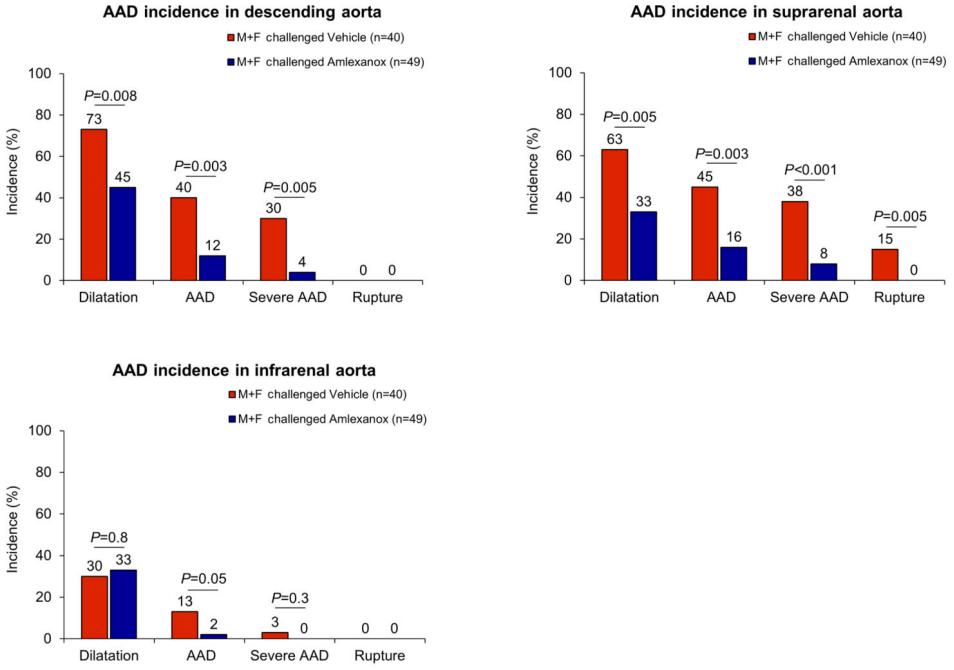

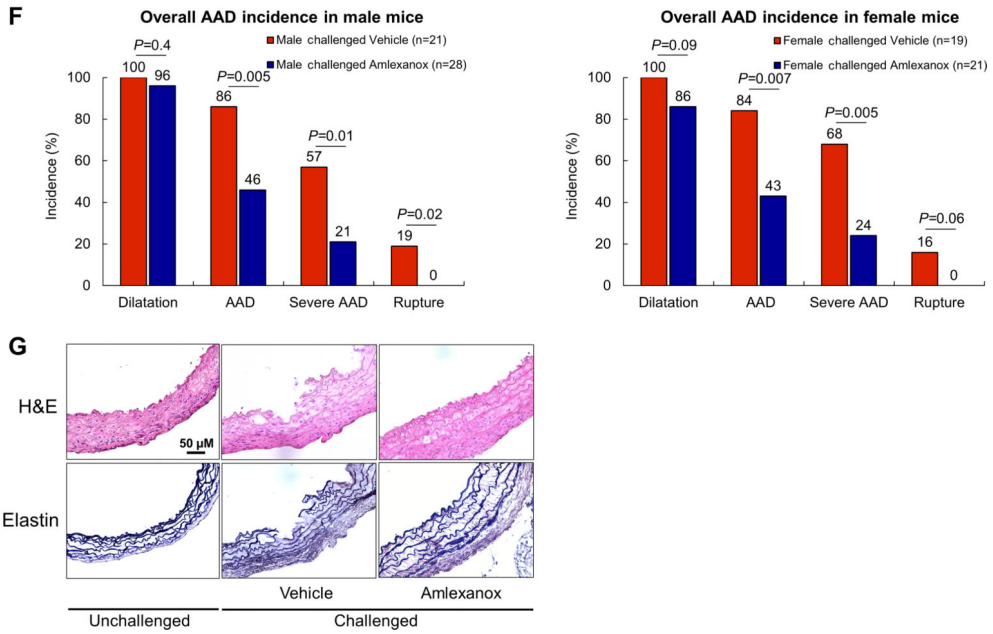

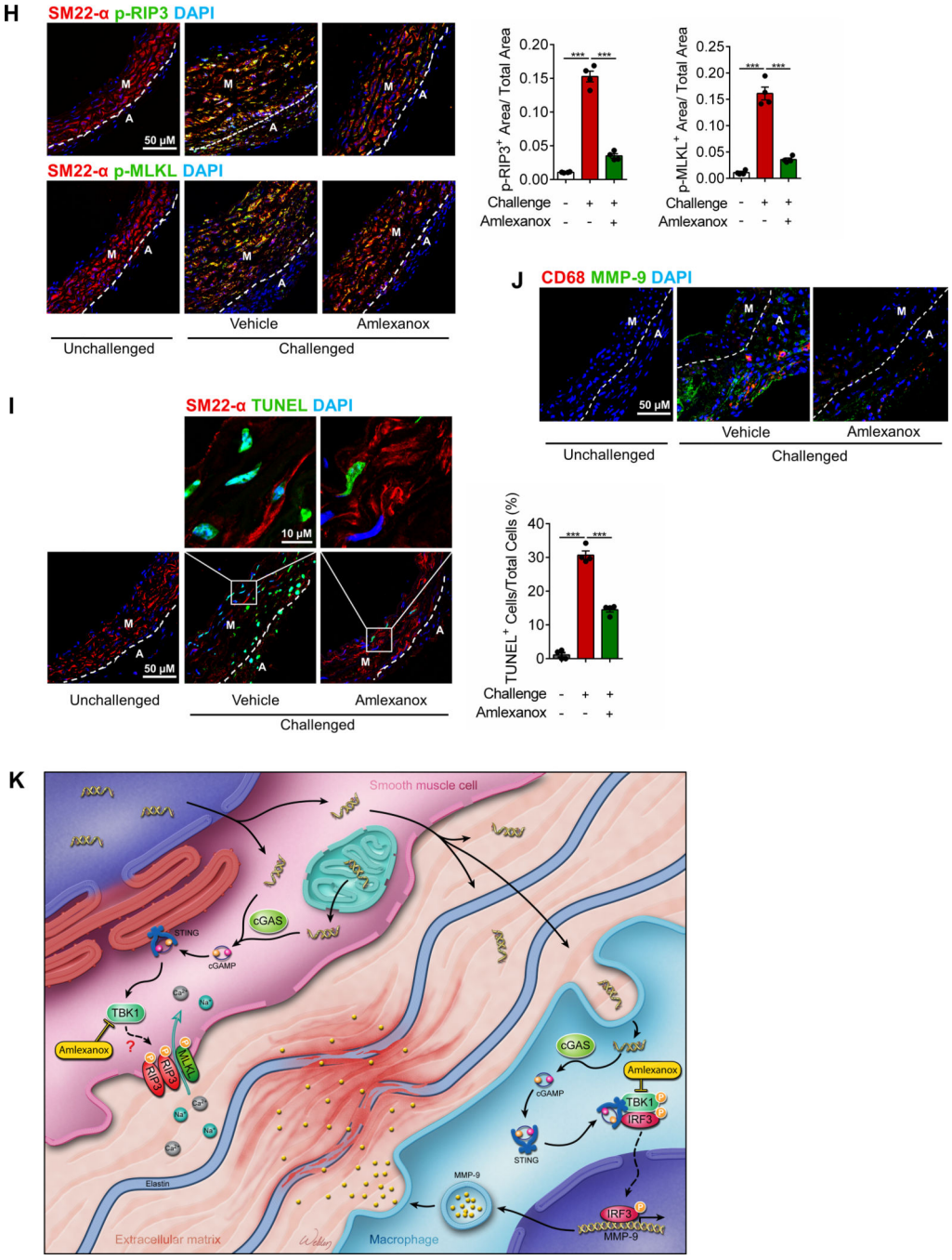

Figure 8. Attenuation of challenge-induced aortic destruction and aortic aneurysm and dissection (AAD) development in wild-type (WT) mice treated with the STING inhibitor amlexanox.

Male and female WT mice were challenged with a high-fat diet and angiotensin II (AngII; 2000 ng/min/kg) infusion and were given either amlexanox (100 mg/kg dissolved in sunflower oil) or sunflower oil (control) daily by oral gavage during the AngII infusion period. **A**, Excised aortas showing that amlexanox attenuated challenged-induced AAD formation. **B**, Aortic diameters in various segments in both male and female challenged WT mice were reduced with amlexanox treatment. Asc, ascending; Desc, descending; SR,

suprarenal; IR, infrarenal. **C**, The overall incidence of AAD in challenged mice was reduced with amlexanox treatment. **D**, Kaplan-Meier survival analysis showing improved survival at 4 weeks of angiotensin II infusion in challenged mice that received amlexanox. **E**, The incidence of AAD in different aortic segments was significantly lower in mice treated with amlexanox. **F**, The overall reduction of AAD incidence was similar in male and female mice treated with amlexanox. **G**, Hematoxylin and eosin (H&E) staining and Verhoeff–van Gieson elastin staining showing the preservation of aortic structure and elastic lamellar architecture in mice treated with amlexanox. **H**, Representative immunofluorescence staining and quantification showing lower levels of phosphorylated (p)-RIP3 and p-MLKL in aortas from the challenged mice treated with amlexanox (n=4 per group) (M: media; A: adventitia). **I**, Representative terminal deoxynucleotidyl transferase dUTP nick end labeling (TUNEL) staining and quantification showing that SMC apoptosis was decreased with amlexanox treatment (n=4 per group) (M: media; A: adventitia). **J**, Representative immunofluorescence staining showing decreased MMP-9 levels in macrophages (CD68) of aortas from challenged mice treated with amlexanox (M: media; A: adventitia). **K**, A schematic illustration showing that STING activation promotes AAD formation. Stress in SMCs causes DNA damage and the release of DNA from the nucleus and mitochondria into the cytosol. DNA in the cytosol binds to and activates cGAS, which produces cGAMP from ATP and GTP. cGAMP binds and activates STING and subsequently TBK1, leading to necroptotic cell death. The DNA fragments from damaged SMCs are engulfed by macrophages and are converted to cGAMP. cGAMP activates STING and subsequently IRF3, which enters the nucleus, binds to the *MMP9* promoter, and induces MMP-9 expression, leading to extracellular matrix destruction. An unpaired, two-tailed *t*-test was used in **(B)**. One-way ANOVA with the Tukey post-hoc test was used for pairwise comparisons in **(H)** and **(I)**. The Fisher exact test was used for **(C)**, **(E)**, and **(F)**. ***$P<0.001$. Data are presented as the mean ± standard error of the mean.